

# UC Santa Barbara

## UC Santa Barbara Electronic Theses and Dissertations

### Title

A tale of two drivers: exploring the response of the marine diatom, *Thalassiosira pseudonana* to changes in temperature and irradiance

### Permalink

<https://escholarship.org/uc/item/28m0d4h6>

### Author

Sweet, Julia Anne

### Publication Date

2020

Peer reviewed|Thesis/dissertation

UNIVERSITY OF CALIFORNIA

Santa Barbara

A tale of two drivers: exploring the response of the marine diatom, *Thalassiosira pseudonana* to changes in temperature and irradiance

A Thesis submitted in partial satisfaction of the  
requirements for the degree Master of Science  
in Marine Science

by

Julia Anne Sweet

Committee in charge:

Professor Uta Passow, Co-Chair

Professor M. Debora Iglesias-Rodriguez, Co-Chair

Professor Mark Brzezinski

September 2020

The thesis of Julia Anne Sweet is approved.

---

Mark Brzezinski

---

M. Debora Iglesias-Rodriguez, Committee Co-Chair

---

Uta Passow, Committee Co-Chair

September 2020

## DEDICATION

For my husband Matt and my best friend Sarah, who never stop cheering for me.

## ACKNOWLEDGEMENTS

I must begin first and foremost by thanking my wonderful committee, Professor Uta Passow, Professor Debora Iglesias-Rodriguez, and Professor Mark Brzezinski for being so generous with their time, expertise, and guidance over the course of my time at UCSB. You are all exceptional mentors and I look forward to continuing our relationships in the years to come.

I thank the National Science Foundation (NSF) for funding this project, and all the past, present, and honorary members of the Passow lab. I am especially grateful to Dr. Nigel D'Souza, Dr. Sari Giering, Elisa Romanelli, Marianne Pelletier, Chance English and Thummanoon Jenarewong; this project would not have been possible without your ongoing support both in and out of the lab and your contagious passion for science.

Last but certainly not least, I thank my amazing parents, husband, and support system of friends (including our dog Sawyer), for providing the comic relief, pep-talks and shoulders to cry on required to complete this journey to my long-awaited goal of obtaining a graduate degree.

## ABSTRACT

A tale of two drivers: exploring the response of the marine diatom, *Thalassiosira pseudonana* to changes in temperature and irradiance

by

Julia Anne Sweet

As human induced climate change continues to alter the world's oceans, it becomes increasingly important to hone the predictive power of models to understand the ecosystem level changes and challenges that the coming decades will bring. However, models are only as robust as the data upon which they are formulated, and the experimentation required to inform them must be based on an interconnected and concomitantly changing set of conditions. Phytoplankton, specifically diatoms, are a worthy focus group as they are particularly ecologically successful—and responsible for approximately 40% of marine primary production. By scrutinizing the potential effects of climate change on phytoplankton, the base of the marine food web, researchers can obtain crucial information upon which to build predictions for entire ecosystems.

This series of experiments was designed to investigate the combined effects of temperature and light on the growth and photophysiology of two strains (one coastal and one open-ocean) of the diatom *Thalassiosira pseudonana*. The goal in producing this data-set is to add to the growing body of multi-stressor research which will aid in understanding the response of phytoplankton to future ocean conditions. This set of experiments takes advantage of advances in culturing techniques and utilizes a bioreactor (multicultivator Z160-OD) containing individual treatment vessels, thus allowing for the easy cultivation of

diatoms under eight different light regimes at the same temperature. Through the use of higher treatment numbers across a gradient of conditions, we exploit the opportunity to detect and quantify potential non-linear response patterns.

Our results show that the response of *T. pseudonana* to simultaneous changes in temperature and irradiance is dependent on the measured response trait, which suggests that interpretation of performance curves requires clear identification of all conditions under which they were generated. Our data also suggest subtle differences between the two strains in the response of growth rate at suboptimal irradiances. Over the range of temperatures tested in these experiments where growth was possible, temperature proved unimportant to the growth rate of the open ocean strain (CCMP 1014) at suboptimal light levels. Whereas the coastal strain (CCMP 1335) demonstrated an interactive relationship between light and temperature at suboptimal irradiances. As temperatures were pushed above the optimal, the cellular characteristics of carbon content and size of the open ocean strain exhibit a clear split based upon irradiance; with high light leading to large carbon-poor cells and low light resulting in small, carbon-dense cells. Our findings also support the idea that the relationship between growth rate and cellular carbon content, while complex and non-linear, is likely predictable. The “choices” and energy trade-offs employed by this species of diatom under the simplified set of experimental conditions in this study, highlight the importance of having clear understandings of the mechanisms driving these changes before they are incorporated into models, as hypothetical outcomes could be missed if only values obtained under specific ranges are used for prediction.

## TABLE OF CONTENTS

1. Introduction.....	1
1.1 The multifaceted nature of ocean change.....	1
1.2 Why study phytoplankton .....	2
1.3 The value and challenge of multistressor research .....	4
1.4 Design and goals.....	4
1.5 Driver one: Temperature .....	5
1.6 Driver two: Irradiance .....	7
2. Methods .....	8
2.1 Experimental Design.....	8
2.2 Culture Media .....	9
2.3 Daily Sampling .....	10
2.4 Flow Cytometry .....	11
2.5 Photophysiology .....	11
2.6 Chlorophyll and Particulate Organic Carbon .....	13
2.7 Nutrient Chemistry.....	13
2.8 Carbonate Chemistry Analysis .....	14
3. Results .....	15
3.1 Experimental Conditions.....	15
3.2 Growth Rates .....	15
3.3 Maximum Quantum Yield of Photosystem II .....	17
3.4 Maximum Relative Electron Transport Rates .....	17



3.5 Cellular Carbon.....	18
3.6 Cellular Chlorophyll .....	19
3.7 Estimated Spherical Diameter .....	20
4. Discussion .....	21
4.1 Achieving the goals of this study.....	21
4.2 From the coast to the open ocean: Key difference between strains...	21
4.3 Comparisons to previous work .....	25
4.4 Links between cell size, carbon content and growth rate.....	28
4.5 Conclusions .....	30
5. References .....	33
6. Figures .....	43

## LIST OF FIGURES

### **Figure 1.**

Ocean acidification, warming, and deoxygenation associated with increasing atmospheric CO<sub>2</sub> rise. Shoaling of the upper mixed layer (UML) due to warming exposes organisms dwelling there to higher levels of solar radiation.

### **Figure 2.**

Image of the multicultivator Z160-OD used in these experiments

### **Figure 3.**

From Eppley 1972 demonstrating (A) the classic relationship between growth rate and temperature and (B) differences in optimal temperature between species.

### **Figure 4.**

Graphics from Steel 1967 and Jassby and Platt 1976 illustrating typical relationships between photosynthesis and light

### **Figure 5.**

Growth rates of the open ocean strain as they relate to (A) irradiance and (C) temperature, and growth rates of the coastal strain as they relate to (B) irradiance and (D) temperature,

### **Figure 6.**

Relationship between quantum yield and irradiance for (A) Open ocean strain and (B) Coastal strain

### **Figure 7.**

Relationship between relative electron transport rates and irradiance for (A) Open ocean strain and (B) Coastal strain

**Figure 8.**

Relationship between cellular carbon content and irradiance for (A) Open ocean strain and (B) Coastal strain

**Figure 9.**

Relationship between cell size (ESD) and irradiance for the open ocean strain

**Figure 10.**

Relationship between cell size (ESD) and growth rate for the open ocean strain, (A) in terms of temperature and (B) in terms of irradiance

**Figure 11.**

Relationship between cell size (ESD) and cellular carbon content for the open ocean strain, (A) in terms of temperature and (B) in terms of irradiance.

**Figure 12.**

Relationship between cellular carbon content and growth rate for (A) the open ocean strain and (B) the coastal strain.

**Table 1.**

Chart of experimental conditions for each strain of *Thalassiosira pseudonana*

**Table 2.**

Definitions of biologically relevant temperature and irradiance cutoffs based upon the growth rate data from this study

**Table 3.**

Table of results comparisons between the two different strains of *Thalassiosira pseudonana*.

# INTRODUCTION

## 1.1 The multifaceted nature of ocean change

Human activities continue to increase the concentration of carbon dioxide (CO<sub>2</sub>) in our planet's atmosphere. The impact of this anthropogenic CO<sub>2</sub> on the world's oceans is two-fold, leading to both warmer sea surface temperatures and a shift in ocean chemistry. While the ocean can act as a sink for some anthropogenic carbon dioxide, removing roughly 31% (Gruber et al., 2019), this amelioration comes at a cost, reducing ocean pH and causing shifts in seawater carbonate chemistry in the well know process of ocean acidification (OA) (Doney et al., 2009). The warming associated with the increase in the partial pressure of carbon dioxide ( $p\text{CO}_2$ ) is expected to raise the average sea surface temperature by 1-4°C (Feng et al., 2009; Hare et al., 2007). The warming climate influences regional and wind patterns and thus ocean circulation in multiple dimensions (Doney et al., 2012). Additionally, rising ocean temperatures can lead to increased thermal ocean stratification, by reducing mixing and ventilation and causing a shoaling of the mixed layer (Bopp et al., 2013; Gao et al., 2019) (Figure 1). This may have indirect effects on the organisms inhabiting the euphotic layer by reducing nutrient supply and altering irradiance exposure (Bopp et al., 2013; Boyd et al., 2008; Gao, Helbling, et al., 2012; Gao, Xu, et al., 2012). The complex task of identifying the impacts of these of concomitant ocean changes, from local to global scales, is critical in order to guide policy-making and make accurate predictions of the future marine biosphere (Boyd et al., 2018).

## 1.2 Why study phytoplankton?

Phytoplankton can be thought of a lifestyle in addition to being a type of organism. The term comes from the Greek roots *phyto* (plant) and *plankton* (to wander or drift), some phytoplankton are bacteria, some are protists, and most are single-celled photoautotrophs (Lindsey et al., 2010). Just like their terrestrial counterparts, phytoplankton capture sunlight and use photosynthesis to turn it into chemical energy thus consuming carbon dioxide and releasing oxygen. In addition to their production of roughly half of the biologically formed oxygen in our atmosphere, phytoplankton are responsible for the cycling of critical elements such as carbon, nitrogen and phosphorus as well as playing a crucially important role in marine food webs, atmospheric exchanges, and carbon sequestration via the biological pump (Sarhou et al., 2005). One main class of phytoplankton—diatoms are particularly successful ecologically, and responsible for 40% of marine primary production (Nelson et al., 1995). Therefore, studying the effects of climate change on these marine primary producers can provide a useful window into how interweaving drivers can affect entire systems via bottom up controls.

In marine environments, abiotic conditions such as temperature, pH, light, and nutrients naturally fluctuate through time, occasionally passing thresholds that induce physiological stress (Gunderson et al., 2016). The growth of diatoms is dependent upon a combination of abiotic factors such as temperature, light, salinity and biotic factors including competition, predation, and infection. Common measures of diatom health and functionality include photosynthesis, growth rate, and respiration. The ocean biome is dynamic, and phytoplankton constantly find themselves exposed to a wide variety of environmental conditions globally, while locally experiencing seasonal cycles of mixing and upwelling. A

particular species or strain of phytoplankton is able to function optimally over a specific and finite range of environmental conditions. When it finds itself outside of these conditions, it is said to be stressed, and the threshold level of stress is usually associated with macromolecular damage requiring energy expenditures for repair (Gunderson et al., 2016; Passow & Laws, 2015). The term “stressor” is only really appropriate when a driver of growth reaches one of these thresholds and while the response of that condition is yet to be determined the term driver is more fitting (Henson et al., 2017). Under optimal conditions, the carbon flux for the synthesis of diatom cell macromolecules is in equilibrium with the energy flux provided by photosynthesis; however, changing environmental conditions (such as increased light or nutrient limitation) can result in a loss of equilibrium between these two fluxes and alter carbon allocations (Jakob et al., 2007; Wagner et al., 2017) which could have cascading repercussions for food webs and export systems.

Poised at the base of the food web, behind the controls of the biological carbon pump, phytoplankton are the small domino positioned to have far reaching ecological impacts depending on which way it falls. The eco-physiological characteristics of the species in the phytoplankton community determine the quality and quantity of primary production that is ultimately transferred up the food web and exported to the deep ocean (Finkel et al., 2010). If phytoplankton experience chronic stress, then higher trophic levels may be forced to consume a lower quality of food, which might restrict the regeneration of limited nutrients in the microbial loop, and over long enough periods of time the composition of upwelling waters may be altered (Finkel et al., 2010).

### **1.3 The value and challenge of multistressor research**

As the number of simultaneous potential stressors acting on our coastal and open ocean waters increases, the statistical probability of any one stressor affecting a critical physiological or ecological process increases even in the absence of mechanistic understanding of the interactions among them (Breitburg et al., 2015). In simplest terms, there are three theoretical types of responses to multiple sources of stress: additive, antagonistic, or synergistic (Todgham & Stillman, 2013). An additive effect occurs when the combined effect of multiple stressors equals the summation of the effects of each stressor alone. An antagonistic effect occurs when the combined effect of multiple stressors is smaller than the expected additive effects in isolation. Finally, a synergistic effect occurs when the combined effect of multiple stressors is greater than the expected additive effects of the stressors in isolation (Gunderson et al., 2016; Todgham & Stillman, 2013). Precisely because effects of stressors are often non-additive, the design and interpretation of research involving multiple stressors is complex (Breitburg et al., 2015). Synergistic effects are more likely to be observed when an additional stressor occurs in quick succession or simultaneously to the first source of stress. In these cases the second stress is contributing either to the magnitude or the duration of the stress event, thereby overwhelming response systems (Gunderson et al., 2016).

### **1.4 Design and goals**

The power to predict the responses of phytoplankton taxa to the many changes the oceans will experience in the coming decades requires a suite of approaches to build the necessary body of knowledge, and is well underway (Gao et al., 2019). Environmental observations, controlled experiments both in the laboratory and in situ, and sophisticated

modeling techniques are three approaches that build off each other to help better understand the interactions between changing climate and ocean ecosystems. Small, laboratory incubations can be used to test individual species in controlled, single or multiple stressor experimental conditions. However, the multi-factorial design required for such experiments can very easily result in a number of treatments and replicates that makes the experiment challenging to conduct.

This set of experiments takes advantage of advances in culturing techniques and utilizes a bioreactor (multicultivator Z160-OD) (Figure 2) containing eight individual treatment vessels; this allows for the easy cultivation of diatoms under eight different light regimes at the same temperature. Through the use of four multicultivator units, this study sets out to determine the response of the marine diatom, *Thalassiosira pseudonana* to changes across gradients of temperature and irradiance to gain mechanistic understanding of the interactive and potentially non-linear responses, adding to the body of knowledge being used for prediction.

### **1.5 Driver One: Temperature**

Temperature can affect phytoplankton over a range of scales—from microscopic cellular processes to water column stratification—and is a key element in determining everything from distribution, productivity, and phenological indices (bloom timing and duration), to the diversity and community structure of phytoplankton (Barton et al., 2016; Behrenfeld et al., 2006; Finkel et al., 2010; Gittings et al., 2018; Thomas et al., 2012).

Temperature changes affect organisms directly by altering their metabolic rates (Brown et al., 2004). On the cellular level, temperature effects are usually seen in the cell's ability to alter enzyme-mediated biochemical processes (Berges et al., 2002). Increases in



temperature are known to increase the response time of metabolic pathways, such as those involved in Rubisco, an enzyme required in the first major step of carbon fixation (Helbling et al., 2011). Furthermore, temperature increases may change different metabolic rates of phytoplankton unequally, enhancing respiration rates more than photosynthesis, potentially leading to declines in net oceanic carbon fixation (Lopez-Urrutia et al., 2006; Regaudie-De-Gioux & Duarte, 2012).

Indirectly, temperature change can affect the very structure and composition of the water column, with warming predicted to cause a shoaling of the mixed layer, decreases in dissolved oxygen and exposure of phytoplankton to changes in light and nutrient availability (Gao et al., 2019; Gao, Helbling, et al., 2012; Gao, Xu, et al., 2012; Hutchins & Fu, 2017). This complexity makes the effects of temperature shifts difficult to reconcile. On a global scale, warmer surface water and steeper vertical temperature gradients have been linked to lower oceanic biomass and productivity (Behrenfeld et al., 2006; Doney, 2006). However, in shallow coastal systems, rising temperature has been shown to be the main driver of phytoplankton blooms across species (Trombetta et al., 2019).

Cellular growth responses to changes in temperature are characterized by thermal tolerance curves also called reaction norms (Thomas et al., 2012), and responses of phytoplankton growth rate to changes in temperature have been well documented. In 1972 Eppley demonstrated that variation in growth rates due to temperature in unicellular algae results in a predictable curve shape, and an expression can be written to determine the maximum expected growth rates for temperature conditions under 40°C (Figure 3A). Eppley further demonstrated that these growth rate curves varied greatly between species, that optimum growth temperatures were species specific, and that temperatures in excess of the

optimum for growth (supra-optimum) result in a much steeper decline in growth rate than decreases towards the suboptimal temperature range (Figure 3B) (Eppley, 1972). More recently, Baker and co-authors presented the notion that each type of phytoplankton functional trait, be it a morphological trait like cell size, or physiological trait such as photosynthesis, exhibits a unique thermal performance curve which varies in shape, optimum, and differs from that of growth rate (Baker et al., 2016).

### **1.6 Driver Two: Irradiance**

Faced with dynamic irradiance changes both spatially and temporally, phytoplankton have developed an array of interrelated cellular mechanisms allowing them to optimize light harvesting and utilization (Dubinsky & Stambler, 2009). Phytoplankton are capable of adjusting to their environment by altering the structure and composition of their photosynthetic apparatus (Falkowski & Owens, 1980; Falkowski et al., 1981). Light availability is an absolute necessity for photosynthesis, but excessive visible and UV radiation impair productivity (Hader & Gao, 2015). Therefore, photoautotroph evolution has had to walk the line between harvesting the maximum amount of light for photosynthesis and minimizing the potential for damage caused by over-excitation of the photosynthetic apparatus (Long et al., 1994; Zhu & Green, 2010). Phytoplankton can be subjected to such high irradiance conditions that their light-harvesting capacity exceeds their light processing capacity (Janknecht et al., 2009). A consequence of this is that over-reduced electron transport chains of the photosystems can leak electrons onto O<sub>2</sub>, creating reactive oxygen species (Asada et al., 1974; Gechev et al., 2006; Mehler, 1951). These reactive oxygen

species can be very damaging, leading to decreased photosynthetic performance or even loss of viability (van de Poll et al., 2005).

The relationship between photosynthesis and irradiance is often presented as a light response curve, or photosynthesis-energy (PE) curve (Steele 1967, Jassby and Platt 1976) (Figure 4) and describes the biomass specific rate of photosynthesis as a saturating function of irradiance (Geider et al., 1997). While the general shape of response curves to increasing irradiance levels are very well known, the specific values vary enormously across phytoplankton species, with optimal irradiance for growth ranging from 20 - 1000  $\mu\text{mol photons m}^{-2}\text{s}^{-1}$ , and maximum growth rate ranging from 0.1- 3.8  $\text{day}^{-1}$  (Edwards et al 2015). Furthermore, responses to changing irradiances can vary depending on the magnitude, duration, and direction of the change (Post et al 1985).

## 2. METHODS

### 2.1 Experimental Design

This series of experiments was designed to investigate the combined effects of temperature and light on the growth and photophysiology of two strains of the diatom *Thalassiosira pseudonana*. Culture Collection of Marine Phytoplankton (CCMP) strain 1014 and CCMP strain 1335 were obtained from Bigelow National Center for Marine Algae and Microbiota and represent an open ocean strain and a coastal strain respectively. Experiments were conducted in multicultivator MC-1000 OD units (Photon Systems Instruments, Drasov, Czech Republic). Each multicultivator unit consists of eight 85 ml test-tubes immersed in a temperature-controlled water bath, each independently illuminated by an array of cool white LEDs. For these experiments, the multicultivator unit was set to the desired incubation

temperatures of 15°C, 18°C, 22°C, and 26°C for CCMP 1335 and 13.5°C, 20°C, 25°C, 29°C, 31°C, and 32.5 °C for CCMP 1014. These temperatures were selected based upon literature reporting thermal tolerance and optima in each strain (Boyd et al., 2013) as well as pre-experiments conducted in the multicultivator. Within each multicultivator, each of the eight test tubes was independently exposed to a different irradiance, ranging from 30 to 265  $\mu\text{mol photons m}^{-2} \text{ s}^{-1}$  for CCMP 1335 and from 25 to 600  $\mu\text{mol photons m}^{-2} \text{ s}^{-1}$  for CCMP 1014 (See Table 1 for chart of experimental conditions). All incubations were performed using 12hr light and 12hr dark cycles. Bubbling of 0.2  $\mu\text{m}$  filtered ambient air into the culture vessels was kept low but continuous to prevent  $\text{CO}_2$  limitation. Each experiment was split into two phases. First, an acclimation phase spanning 3 days (equivalent to 1-5 generation times) was used to allow cultures to adjust to their respective temperature and light regimes. Next, pre-acclimated, exponentially-growing cultures were inoculated into fresh media and incubated for a 4-day experimental phase during which assessments of growth and photophysiology were carried out daily. All sampling was conducted 6 hours into the daily light cycle to minimize effects of diurnal cycles. Data shown in this study are averages over a 48-hour period ( $n = 3$  daily samples) spanning day 0 to day 2 of the experimental phase during which cultures were experiencing exponential growth. For experiments with CCMP 1335, the particulate organic carbon and chlorophyll results presented are averages of day 1 and day 2, as no day 0 samples were taken.

## 2.2 Culture Media

The strains used in this study were grown in artificial seawater (ASW) (Kester et al., 1967), which was enriched with 50 mL of sterile filtered, UV treated natural seawater per

liter of ASW. Results from previous experiments had shown that after a few weeks this species does not grow well in ASW media, suggesting the need for some unknown trace element. The carbonate chemistry was adjusted by adding  $\text{NaHCO}_3$  to reach a DIC of  $2050 \mu\text{mol kg}^{-1}$  and by adding NaOH to reach the target pH values of  $8.0 \pm 0.1$  (Passow, 2012). This growth medium was then enhanced with *f/2* nutrients (Guillard, 1975) to avoid nutrient limitation.

Sterilization techniques for the natural seawater (added to the ASW media) were investigated to determine the best method to avoid disruption of the natural carbonate chemistry of the natural seawater. To determine this, pH and DIC samples from autoclaved and UV-sterilized media were compared. These comparisons demonstrated that sterilization via UV light was a superior technique for preserving the natural carbonate chemistry, and was utilized for treatment of the natural seawater component of the growth media.

### **2.3 Daily Sampling**

During sample collection each tube was gently, but thoroughly mixed, and subsampled for the assessment of cell density and photophysiology. The former samples were fixed with hexamethylenetetramine-buffered formaldehyde (final concentration 1% v/v) and stored at  $4 \text{ }^\circ\text{C}$  in the dark for a maximum of 4 days before flow cytometry analysis, while the latter were dark adapted prior to photophysiology measurements. Following a 30-minute dark adaptation and non-destructive measurements of photophysiology (see below), samples were filtered for chlorophyll *a* (Chl *a*) and particulate organic carbon (POC) determinations. On the last day of the experimental phase, nutrient samples were collected to assess possible limitations.

## **2.4 Flow Cytometry**

Samples were analyzed on a Guava easyCyte HT Benchtop Flow Cytometer (Millipore-Sigma, USA), and a minimum of 200 cells per sample enumerated. All data acquisitions were done with logarithmic signal amplification, and low cytometer sample flow rates ( $0.24 \mu\text{L s}^{-1}$ ) in order to accommodate high cell density. Diatoms were identified based on size and chlorophyll autofluorescence using the forward scatter channel (FSC) and Red-FL (695/50 nm) channel respectively. Samples from CCMP 1014 treatments grown at  $25^\circ\text{C}$  and  $25 \mu\text{mol photons m}^{-2} \text{s}^{-1}$ , and  $25^\circ\text{C}$   $50 \mu\text{mol photons m}^{-2} \text{s}^{-1}$  were lost, and no cell counts are reported.

Growth rates ( $\mu$ ) were determined by fitting an exponential curve to a plot of cell abundance vs. time for the 48-hour period of the experimental phase during which cells exhibited exponential growth (in all cases this was days 0 through 2). Growth rates in treatments where cells either did not grow, or declined in abundance were logged as 0. Cell sizes (equivalent spherical diameter (ESD) in  $\mu\text{m}$ ) were derived from forward scatter measurements (FSC) using size-calibration beads of known diameters ranging from  $2 \mu\text{m}$  to  $10 \mu\text{m}$  (Particle Size standard kit, Spherotech Inc.).

## **2.5 Photophysiology**

Photophysiology was evaluated daily using the light curve protocol LC3 of a handheld Pulse Amplitude Modulated (PAM) fluorometer (AquaPen-C AP-C 100, Quibit Systems, Ontario, Canada). Light curves provided in-vivo chlorophyll autofluorescence ( $F_0$ ),

the maximum quantum yield ( $QY_{max} = F_v/F_m$ ) and relative photosynthesis rates based on PSII quantum yields (rETR) at varying irradiances.

Where,

$F_0$  = Minimum fluorescence yield

$F_m$  = Maximum fluorescence yield during the saturating flash

$F_v$  = Variable fluorescence ( $F_m - F_0$ )

Consalvey et al. (2005). The LC3 protocol involves measurements of baseline and maximal fluorescence over seven 60-second phases, with each phase representing an irradiance from 10 to 1000  $\mu\text{mol photons m}^{-2} \text{s}^{-1}$ . Blue light (455 nm) was used as actinic light in these experiments, and measurements were made at measuring illumination (f-pulse) intensity of 0.03  $\mu\text{mol photons m}^{-2} \text{s}^{-1}$ , and saturating (F-pulse) illumination of 2100  $\mu\text{mol photons m}^{-2} \text{s}^{-1}$ . Actinic illumination (A-pulse) controlled by the instrument's protocol were set at 10, 20, 50, 100, 300, 500, and 1000  $\mu\text{mol photons m}^{-2} \text{s}^{-1}$  (for each 60-second phase). The PSII quantum yields at these irradiances were used to generate relative electron transport rates (rETR), using the formula:

$$\text{rETR} = [(F_{m\_L_n} - F_{t\_L_n})/F_{m\_L_n}] \times [(\text{irradiance})/2]$$

Where,

$F_{m\_L_n}$  = Maximum fluorescence in light adapted state

$F_{t\_L_n}$  = Instantaneous fluorescence during light adaption

n = represents a sequential number of light phase

In the above equation, “irradiance” refers to the actinic light intensity corresponding to the respective  $L_n$ , and the irradiance is divided by 2, based on the assumption that photons divide equally between PSI and PSII (Consalvey et al., 2005).

## **2.6 Chlorophyll and Particulate Organic Carbon**

For chlorophyll analysis, 3 ml sample aliquots were filtered onto 0.45  $\mu\text{m}$  mixed cellulose filters, folded into thirds and stored at  $-20^\circ\text{C}$ . Filters were placed in 90% acetone (v/v) overnight at  $-20^\circ\text{C}$ , and the extracted chlorophyll was measured fluorometrically on a Turner 700 fluorometer (Strickland & Parsons, 1972). Chlorophyll-a liquid standards in 90% acetone (Turner Designs Inc.), and adjustable solid secondary standards (Turner Designs Inc. P/N 8000-952) were used for calibrations.

3 mL samples for particulate organic carbon (POC) were filtered onto 25mm pre-combusted glass fiber filters (GF/F), dried at  $60^\circ\text{C}$ , then stored at room temperature until analyses. Samples were analyzed using an elemental analyzer (CEC 44OHA; Control Equipment). Carbon content was normalized to cell abundance to assess cellular carbon content across treatments.

## **2.7 Nutrient chemistry**

Nutrient samples were taken from the media at the start of each phase of the experiment, and from each treatment on the terminal day of the experiment. Samples for nutrient analysis were filtered through 0.2  $\mu\text{m}$  filters into clean plastic bottles and stored at  $-20^\circ\text{C}$  until analyses for nutrients. Phosphate ( $\text{PO}_4$ ), nitrate ( $\text{NO}_3$ ) + nitrite ( $\text{NO}_2$ ), and silicic acid ( $\text{Si}(\text{OH})_4$ ) were measured by Flow injection analysis (FIA) using a QuikChem 8500 Series 2 AutoAnalyzer (Lachat Instruments, Zellweger Analytics, Inc.).



## 2.8 Carbonate Chemistry Analysis

The pH (total scale) was measured with a spectrophotometer (Genesys 10SVIS) using the indicator dye m-cresol purple (Sigma Aldrich) at 25 °C. The absorbance was measured at 730 nm, 578 nm, and 434 nm before and after dye (Clayton & Byrne, 1993; Fanguie et al., 2010). A TRIS buffer solution in synthetic seawater with known pH, supplied by A. Dickson (Scripps Institution of Oceanography, USA) was used to calibrate the dye.

For DIC analysis, samples were siphoned into clean glass serum vials, fixed with HgCl<sub>2</sub> (0.035 % final conc. v/v), and sealed with butyl rubber septa. Samples were stored at 4°C prior to analysis and were always processed within 30 days. DIC samples were analyzed using an automated infrared inorganic carbon analyzer (AIRICA). Multiple injections for each sample gave replicate values per sample that were averaged. The AIRICA-23 (MARIANDA, Kiel, Germany), is a high precision instrument used to measure total dissolved inorganic carbon in seawater. The analyzer uses a high-precision syringe and a mass flow controller to deliver an established volume of sample into a stripper, where it is acidified and transferred to a nondispersive infrared detector. The *p*CO<sub>2</sub> is then measured by a LICOR-7000 gas analyzer using the difference in infrared absorbance between a sample and reference cell. The time integrated *p*CO<sub>2</sub> value is proportional to the amount of dissolved inorganic carbon evolved from the sample and converted to carbon units based on a calibration against a certified reference (Dickson et al., 2007). The carbon units are converted to gravimetric units (μmol/kg) using the weight, temperature, and salinity of the sample. To ensure stability of the instrument, the pH of the certified reference material was measured every 5 samples.

## 3. RESULTS

### 3.1 Experimental Conditions

Throughout the course of this experiment, temperature and light conditions were held consistent to those values prescribed in the methods section. Set irradiance values were measured using a QSL-100 PAR sensor from Biospherical Instruments Inc., and temperature was recorded continuously by the multicultivator unit, checked daily with an independent thermometer, and found to be within (+/-) 3% of the target temperature.

The three-day acclimatization phase of these experiments was designed to allow cultures to adjust to their distinct temperature and light regimes prior to analysis of their growth and photophysiology during the four-day experimental phase. Although samples for cell concentration were taken during the acclimatization period to identify exponential growth, all results presented are from a 48hr period of the experimental phase.

While the use of a three-day acclimatization period avoided measuring the immediate stress response, it is possible that cells in treatments that generated slower growth rates may not have not have been fully acclimatized to their respective conditions by the end of this phase.

### 3.2 Growth Rates

#### **Open ocean strain: CCMP 1014**

For this strain, the maximum growth rate of  $1.9 \text{ day}^{-1}$  was recorded in the treatment exposed to  $25 \text{ }^{\circ}\text{C}$  and  $600 \mu\text{mol photons m}^{-2} \text{ s}^{-1}$ , and the lowest (measurable) growth rate of  $0.3 \text{ day}^{-1}$  was observed in the culture grown at  $13.5^{\circ}\text{C}$  and  $25 \mu\text{mol photons m}^{-2}\text{s}^{-1}$ . As

irradiance levels were increased from 25 and 190  $\mu\text{mol photons m}^{-2} \text{s}^{-1}$ , all temperatures (with the exception of 32.5 °C) demonstrated a positive linear increase in growth rate. Below 190  $\mu\text{mol photons m}^{-2} \text{s}^{-1}$  temperature had very little effect and growth rate increases were driven by light. Between 190 and 600  $\mu\text{mol photons m}^{-2} \text{s}^{-1}$  light saturation set in and growth rates show very little change with increasing irradiance within each temperature regime (Figure 5A). Growth rates indicate that the optimal temperature for this species lies between 20°C and 25°C and growth was completely inhibited at 32.5°C (Figure 5C).

#### **Coastal strain: CCMP 1335**

The highest growth rate of 1.6  $\text{day}^{-1}$  was obtained from the culture grown at 26°C and 265  $\mu\text{mol photons m}^{-2} \text{s}^{-1}$ , whereas lowest growth rate of 0.4  $\text{day}^{-1}$  was observed in the culture grown at 15°C and 30  $\mu\text{mol photons m}^{-2} \text{s}^{-1}$  (Figure 5B). After irradiance levels reach around 125  $\mu\text{mol photons m}^{-2} \text{s}^{-1}$ , light saturation effects are seen with very slight responses in growth rate to increasing irradiance levels. Below 70  $\mu\text{mol photons m}^{-2} \text{s}^{-1}$  temperature had little effect on growth rate, and cell division appears only light dependent (light limited) (Figure 5D). However, for irradiances of 70  $\mu\text{mol photons m}^{-2} \text{s}^{-1}$  and above, there is a significant linear correlation between increasing temperature and increasing growth rate at each given light regime (Pearson's two tailed test  $p < 0.01$   $n=4$ ). Growth rate increases by 0.03 to 0.06 per degree Celsius, with the steepest slope recorded at 105  $\mu\text{mol photons m}^{-2} \text{s}^{-1}$  (Figure 5D). The range of temperatures used to test this strain of *T. pseudonana* did not extend to a value that inhibited growth completely, and based on the obtained growth rate values, the optimum temperature for this species is located at 26°C or warmer.

### **3.3 Maximum Quantum Yield of Photosystem II ( $QY_{max}$ )**

#### **Open ocean strain: CCMP 1014**

The maximum quantum yield of photosystem II  $QY_{max}$ , can be used to assess cell health, with values above 0.6 typically indicating that diatoms are not experiencing stress (Kromkamp & Peene, 1999).  $QY_{max}$  values for this species ranged from 0.61 to 0.76 across all temperature-irradiance settings tested. A strong linear relationship between increasing light levels and decreasing quantum yield values (Pearson's two tailed test  $p < 0.01$   $n=8$ ) existed in all treatments except those cultured at 13.5°C, which exhibited consistently high  $QY_{max}$  values across all irradiances (Figure 6A). The temperature light combination (25 °C 600  $\mu\text{mol photon m}^{-2} \text{s}^{-1}$ ) in which the maximum growth rate was recorded exhibited the lowest  $QY_{max}$  value.

#### **Coastal strain: CCMP 1335**

A small range of maximum quantum yield values, from 0.68 to 0.74, was observed for all treatments, with the highest  $QY_{max}$  values recorded at 22°C. However, the observed spread in  $QY_{max}$  may not be statistically different, implying that over the range of conditions tested there was no temperature or irradiance effect on  $QY_{max}$  (Figure 6B).

### **3.4 Maximum Relative Electron Transport Rates ( $rETR_{Max}$ )**

#### **Open ocean strain: CCMP 1014**

$rETR_{max}$  measures the relative electron transport rates between PSII and PSI, and can be used as a proxy for primary productivity (Bretherton et al., 2018; Consalvey et al., 2005).

For this strain of *T. pseudonana*,  $rETR_{max}$  values ranged from 54 relative units to 105 relative units, but did not exhibit clear trends with irradiance or temperature (Figure 7A).

#### **Coastal strain: CCMP 1335**

For the coastal strain,  $rETR_{max}$  ranged from 42.7 to 65.9 relative units, with increasing levels of irradiance producing higher  $rETR_{max}$  values. Temperature may also have had a slight effect at irradiances less than or equal to  $125 \mu\text{mol photons m}^{-2} \text{s}^{-1}$ . At these lower irradiance levels treatments grown at  $22^\circ\text{C}$  exhibit  $rETR_{max}$  values that were 6-30% higher than those seen at other temperatures tested ( $15^\circ\text{C}$ ,  $18^\circ\text{C}$ ,  $26^\circ\text{C}$ ), however once irradiance levels reached  $265 \mu\text{mol photons m}^{-2} \text{s}^{-1}$ , temperature had little or no effect on  $rETR_{max}$  (Figure 7B).

### **3.5 Cellular Carbon**

#### **Open ocean strain: CCMP 1014**

Highest cellular carbon content (Table 3) was recorded at  $31^\circ\text{C}$  and  $25 \mu\text{mol photons m}^{-2} \text{s}^{-1}$ , while the lowest values were noted at  $29^\circ\text{C}$  and  $600 \mu\text{mol photons m}^{-2} \text{s}^{-1}$ . Averaged across all temperature regimes, very low irradiance levels,  $25$  and  $50 \mu\text{mol photons m}^{-2} \text{s}^{-1}$  produced cells whose carbon content was approximately 380% and 174%, higher, respectively, than values seen at irradiances between  $80$  and  $600 \mu\text{mol photons m}^{-2} \text{s}^{-1}$ . At saturating irradiances ( $>190 \mu\text{mol photons m}^{-2} \text{s}^{-1}$ ), treatments in the optimal temperature range of  $20^\circ\text{C}$  to  $25^\circ\text{C}$  exhibited higher cellular carbon content than at other temperatures, but variability overall was high (Figure 8A).

### **Coastal strain: CCMP 1335**

Displaying a similar trend to CCMP 1014, this strain also exhibits a pattern of higher cellular carbon at low irradiances ( $<100 \mu\text{mol photons m}^{-2} \text{s}^{-1}$ ). High variability between treatments make the effects of temperature difficult to discern, except to note that cells grown at  $22^\circ\text{C}$  demonstrated the smallest cellular carbon content across all light conditions (Figure 8B).

### **3.6 Cellular Chlorophyll (Chl *a*)**

#### **Open ocean strain: CCMP 1014**

Highest cellular chlorophyll values ( $0.69 \text{ pg per cell}$ ) were observed in low light treatments ( $25$  and  $50 \mu\text{mol photons m}^{-2} \text{s}^{-1}$ ). However, variability was high and temperature also influenced cellular chlorophyll content. Below  $150 \mu\text{mol photons m}^{-2} \text{s}^{-1}$ , supra-optimal temperatures ( $29^\circ\text{C}$  and  $31^\circ\text{C}$ ) drive cellular chlorophyll content to larger values ( $0.69 \text{ pg per cell}$ ) than those seen at optimal ( $20^\circ\text{C}$ ,  $25^\circ\text{C}$ ) and sub-optimal ( $13.5^\circ\text{C}$ ) temperatures ( $0.24$ -  $0.34 \text{ pg per cell}$ ). Lowest cellular chlorophyll content ( $0.09 \text{ pg per cell}$ ) was recorded in cells incubated at  $13.5^\circ\text{C}$ .

#### **Coastal strain: CCMP 1335**

As with CCMP 1014, highest chlorophyll per cell values ( $0.39$ -  $0.45 \text{ pg per cell}$ ) were observed under low irradiance (below  $100 \mu\text{mol photons m}^{-2} \text{s}^{-1}$ ). However, temperature has a less clear influence on this strain. Between  $90 \mu\text{mol photons m}^{-2} \text{s}^{-1}$  to  $265 \mu\text{mol photons m}^{-2} \text{s}^{-1}$  the highest values of Chl *a*/ cell are recorded at  $22^\circ\text{C}$  ( $0.45 \text{ pg per cell}$ ). The lowest Chl *a* cell<sup>-1</sup> ratios were seen at  $18^\circ\text{C}$  across all irradiances.

### 3.7 Estimated Spherical Diameter (ESD)

#### Open ocean strain: CCMP 1014

Cell size ranged from 5.6 – 8.7  $\mu\text{m}$  (Table 3) depending on both temperature and light. With the exception of the culture incubated at 13.5 °C, which exhibited no irradiance effect, all treatments demonstrated a significant (Pearson's two tailed test  $p < 0.01$  for 31 °C, 29 °C, 20 °C:  $p < 0.05$  for 25 °C) linear increase in size with increasing irradiance between 25  $\mu\text{mol photons m}^{-2} \text{s}^{-1}$  and 300  $\mu\text{mol photons m}^{-2} \text{s}^{-1}$ . Above 300  $\mu\text{mol photons m}^{-2} \text{s}^{-1}$  irradiance does not affect size; however temperature continues to drive ESD with 29 °C and 31 °C producing the largest cell sizes, 20 °C and 25 °C creating medium sized cells and 13.5 °C producing the smallest cells (Figure 9).

When cell size is examined in relation to growth rate, a significant (Pearson's two tailed test  $p < 0.01$ ) positive linear correlation is noted for each temperature greater than 13.5 °C. The slope of this relationship is larger for cultures grown at 29 °C and 31 °C, than for those cultured at 20 °C and 25 °C. The treatment grown at 13.5 °C demonstrated a significant (Pearson's two tailed test  $p < 0.02$ ) negative correlation between size and growth rate (Figure 10).

#### Coastal strain: CCMP 1335

Cell sizes of the coastal strain ranged between 4.6 – 6.6  $\mu\text{m}$  (Table 3), but were likely a function of the population dynamic of the culture, rather than environmental conditions: The average size of a diatom population decreases with age since the last sexual reproduction cycle. For logistical reasons, experiments with this strain were conducted over the span of several months, and starting cell sizes for different temperature trials were

distinct from each other simply due to the timing of the inoculum harvest. Changes with irradiance within each experiment were negligible (data not shown).

## 4. DISCUSSION

### 4.1 Achieving the goals of this study

The goal of investigating the interactive effects of temperature and irradiance at this resolution is to add to the growing body of multistressor research e.g. (Gao et al., 2019; Gunderson et al., 2016) which will facilitate prediction of phytoplankton responses to future ocean conditions. Using two strains of a well-studied, easily cultured diatom species like *Thalassiosira pseudonana* (Armbrust et al., 2004) allows for detailed response comparisons. A major challenge in experimental ecology is to capture the nonlinearities of responses to interacting drivers (Kreyling et al., 2018). In these experiments, by replacing replication with higher treatment numbers in a series that has a well-established response curve (Eppley, 1972; Platt & Jassby, 1976; Steele, 1962), we take advantage of the opportunity to detect and quantify potential nonlinear response patterns while still using a valid statistical approach (Boyd et al., 2018; Kreyling et al., 2018). Additionally, as this study was conducted under nutrient replete conditions, it may also assist in teasing apart the irradiance driven consequences from the nutrient limitation effects of increased stratification (Finkel et al., 2010) in future studies.

### 4.2 From the coast to the open ocean: Key differences between strains

While both the open ocean strain and the coastal strain shared a similar optimal temperature range for maximum growth rates, the open ocean strain was observed to have a



higher saturating irradiance ( $190 \mu\text{mol photons m}^{-2} \text{s}^{-1}$ ) than the coastal strain which experienced light saturation effects at  $125 \mu\text{mol photons m}^{-2} \text{s}^{-1}$  (Table 2). The dynamic mixing and increased turbidity typical in the coastal environment would make the ability to exploit lower light levels very advantageous for a coastal strain. In addition, the growth rate of the open ocean strain did not respond significantly to temperature at sub-optimal irradiance levels, whereas the coastal strain does show an increase of growth rate with temperature increases at sub-optimal irradiances (Table 3). This indicates that at suboptimal irradiance, growth of the open ocean strain is limited by light and not temperature, whereas growth rate of the coastal strain can be driven by both light and temperature. Variability in surface temperature is higher in coastal compared to open ocean waters, and the ability of the coastal strain to grow at suboptimal irradiances would be especially advantageous when coupled with the ability to also harness the benefits of warmer temperatures to accelerate growth.

Growth rates of the coastal strain were thus driven by interactive effects of temperature and light, whereas the open ocean strain switched between dominant drivers with a transition from light to temperature dependent growth above  $190 \mu\text{mol photons m}^{-2} \text{s}^{-1}$ . Diatom species from different habitats frequently differ in their ability to cope with changes in irradiance (Lavaud et al., 2007) and such subtle differences allude to differences in adaptations and energy allocation. Open ocean and coastal phytoplankton communities experience controlling factors and their variability (e.g. nutrients, mixing, iron availability) differently (Trimborn et al., 2015), and therefore allocate energy differently to enhance survival. For example, differences are seen in iron uptake capacity, and carbon

concentrating mechanism's (CCM) between pelagic phytoplankton communities and coastal assemblages (Trimborn et al., 2015).

The maximum relative electron transport rates ( $rETR_{max}$ ) between photosystem II and photosystem I can be interpreted as a proxy for primary production (Bretherton et al., 2018). Low  $rETR_{max}$  values indicate lower generation of NADPH and ATP, which may result in lower growth rates, and/or primary productivity, and may suggest damage beyond Photosystem II (Liu et al., 2015). Using  $rETR_{max}$  values as a proxy for primary production, the open ocean strain appears to perform photosynthesis efficiently over all light ranges and temperatures investigated, whereas  $rETR_{max}$  of the coastal strain was comparably low (Table 3) and increased with irradiance up to the saturation irradiance. Whereas both growth rate and  $rETR_{max}$  of the coastal strain increase with irradiance, and are linearly correlated with each other ( $r^2 = 0.62$ ,  $n=16$ ,  $p=0.02$ ), the insensitivity of  $rETR_{max}$  of the open ocean strain to irradiance and temperature contrasts the respective patterns observed for growth rate.  $rETR_{max}$  and growth rate of the open ocean strain are not at all correlated ( $r^2 = 0.000002$ ,  $n=19$ ). This reveals not only how the response of  $rETR_{max}$  values to temperature and irradiance conditions differs between the strains, but how the definition of 'optimal conditions' depends on the trait under scrutiny.

Generally, high irradiance levels have been linked to lower maximum quantum yields of photochemistry as expressed in  $QY_{max}$  values; this is attributed to the capability of phytoplankton to reduce light-utilization efficiency under high irradiance (the down-regulation of PSII reaction centers) (Consalvey et al., 2005; Goto et al., 2008). Conversely, elevations in temperature have been shown to increase QY (Lassen et al., 2010). This temperature effect is most likely connected to enhanced membrane fluidity, and diffusion

times of electron carriers at higher temperatures (Falkowski & Raven, 1997). However, this positive response of  $QY_{\max}$  with temperature only remains true up to a certain point, once temperatures reach the point of becoming a stressor, a drop in the value of  $QY_{\max}$  can be seen (Bojko et al., 2013). While the open ocean strain showed the expected decrease in  $QY_{\max}$  values with increasing irradiance (except at 13.5°C), the coastal strain showed no statistically significant change with irradiance, and neither strain demonstrated the increase in  $QY_{\max}$  values with increasing temperatures described by other researchers. At suboptimal temperature (13.5°C), and in contrast to all other temperatures, QY of the open ocean strain did not decrease with increasing irradiance either, suggesting a potential offset between light-utilization efficiency and lower temperature. Additionally, the temperature and light conditions for both strains that resulted in maximum growth rates were not the same conditions that produced the highest  $QY_{\max}$  values (Table 3). As maximum quantum yield of photosystem II can and is often used as an effective metric for phytoplankton efficiency and health (Kolber and Falkowski 1993), this again sparks the discussion of exactly what is meant by “optimal” conditions and builds on the suggestion made by Baker et al. (2016), that the optimal temperature for overall fitness is a balance of trade-offs, and growth may not be the best measurement of overall biogeochemical performance.

Energy tradeoffs have been noted before in the architecture of diatom photosystems, where an open ocean diatom species sacrificed its low light harvesting capabilities in return for lower iron requirements (Strzepek & Harrison, 2004) allowing it to thrive in more oligotrophic waters. Even at the strain level, researchers have found substantial variations in how strains of the same species cope with changing environmental parameters (Wolf et al., 2019), prompting highly relevant musings on the concept of culturing strains and how truly

akin they are to their “wild” counterparts (Lakeman et al., 2009). This flexibility of energy allocation in regards to acclimatization and adaptation, while fascinating, adds further layers of complexity to prediction. Our results showcase a variability in short term response patterns within strains of the same species, and thus emphasize the need to address this knowledge gap while modelling responses for entire species or taxa.

#### **4.3 Comparisons to previous work**

The responses of phytoplankton to concurring changes in temperature and irradiance have often been included in studies exploring multiple simultaneous stressors such ocean acidification (Passow & Laws, 2015; Taucher et al., 2015; Wong et al., 2015) or nutrient limitations (Thomas et al., 2017), and the responses have been found to be highly interactive, non-linear, and species and strain dependent. The lack in predictive understanding of such interactive effects is something that our study attempts to shed light on.

As part of our project, the same two strains of *T. pseudonana* used in our study, the open ocean strain CCMP 1014 and the coastal strain CCMP 1335, were also used in two other multistressor experiments: D’Souza and co-authors (2020\*) conducted a three-stressor batch culture experiment, where temperature and irradiance were varied across the range of CCMP 1014’s thermal and light tolerance under three  $p\text{CO}_2$  regimes, and Laws and co-authors (2020), studied the interactive effects of temperature, irradiance, nutrient limitation and  $p\text{CO}_2$  on CCMP 1335 using the continuous culture approach. Their data from cultures grown at ambient  $p\text{CO}_2$  under nutrient replete conditions provides a comparison to our results.

Growth rates of the open ocean strain (CCMP 1014) observed in our experiments were very similar to those seen by D'Souza (2020\*) in their present day  $p\text{CO}_2$  treatments. Despite the fact that we utilized batch culturing for our experiments, the values and trends in growth rates of the coastal strain (CCMP 1335) match very closely to those seen in continuous culture by Laws and co-authors (2020). Li and Campbell (2013), also experimented with this coastal strain of the diatom *T. pseudonana* while determining the interactive effects of light and  $p\text{CO}_2$  on growth, and published graphs of growth rate vs irradiance at 390 ppm which also closely resemble the data produced in our study. Older studies performed by Stramski et al. (2002) used the coastal strain to experiment with the combined effects of temperature, light and nitrogen limitation. While they obtained values for growth rate that were 2- 29% higher than those reached in our experiments, the overall trends of growth in response to temperature and light in their nutrient replete treatments are very similar to those found in our study.

While the general trends of growth rates described in previous studies fit in well with our data, some are performed over a range of temperatures but only under one irradiance condition, while others test many irradiances but only at one temperature. The higher number of treatments in this study allowed not only for more detailed resolution along the growth response curves, but also a clearer comparison between the two strains of this species (Table 3).

It has been demonstrated that responses of photosystem efficiency, pigment compositions and antioxidant activities are highly species specific (Janknegt et al., 2009) so we discuss our findings in relation to studies performed on the same strains of *T. pseudonana*. Results from the open ocean strain in our investigations support the known link

between decreasing  $QY_{\max}$  and increasing irradiance, with the only temperature distinction being greater values at suboptimal (13.5°C) at saturating light levels. However, measurements of  $QY_{\max}$  performed by D'Souza and co-authors (2020\*) found that both increasing temperatures, and irradiance were related to a decrease in  $QY_{\max}$ . While the coastal strain in our study exhibited no significant differences with temperature or irradiance, Laws (2020) reported an increase in  $QY_{\max}$  from 0.56 at 10°C 300  $\mu\text{mol photons m}^{-2} \text{ s}^{-1}$  to 0.68 at 30 °C 300  $\mu\text{mol photons m}^{-2} \text{ s}^{-1}$ . This may be due to the truncated temperature range explored in our study (15-26°C) on this strain in comparison to those explored by Laws (10-30°C).

Examination of  $rETR_{\max}$  values of the open ocean strain in this study do not show any conclusive patterns with light or temperature (Figure 7A). Unlike D'Souza (2020\*), who found  $rETR_{\max}$  values to increase with irradiance but only investigated three irradiances (50, 300, and 600  $\mu\text{mol photons m}^{-2} \text{ s}^{-1}$ ).

Chl *a* concentration is widely used and easily measured index of phytoplankton biomass (Goto et al., 2008). In addition, cellular Chl *a* may indicate changes in physiological responses, driven by light and nutrients (Behrenfeld et al., 2016). An increase in cellular chlorophyll at low light intensities is a common compensation to optimize light harvest (Falkowski & Owens, 1980). Chl *a* has also been shown to decrease with temperature increases, however the signal from chlorophyll is difficult to interpret in situ as it is challenging to separate a response to temperature from a response to the nutrients often present in cooler layers (Behrenfeld et al., 2016; Lassen et al., 2010). Our experiments revealed the expected increase in cellular Chl *a* at low irradiance in both strains, and no significant trends with temperature. These finding are consistent with those from D'Souza

(2020\*) for the open ocean strain, but deviate from those of Stramski et al., 2002 for the coastal strain, who observed lower Chl *a* values (0.4- 0.16 pg cell<sup>-1</sup>) and a clear increase in cellular Chl *a* concentration with increasing temperatures from 7 to 25 °C. Perhaps this discrepancy stems from the small overlap for comparison, as Stramski and colleagues used only one light regime (330-410 μmol photons m<sup>-2</sup> s<sup>-1</sup>), and a wider, shifted range of temperatures (7-25°C) for their exploration.

It is noteworthy that the lowest Chl *a* values in both strains of our study were consistently found in the smallest sized cells, suggesting that cell size is another parameter to consider in this context. If certain combinations of treatment conditions result in a smaller sized cell, then the chlorophyll per cell values may simply be reflecting that size difference. This illustrates again how the conditions for generating large values in one parameter may not hold when another trait is under examination.

#### **4.4 Links between cell size, carbon content and growth rate**

Relationships between temperature, irradiance and cell characteristics often focus on responses to single drivers. Our results allow examination of some cellular characteristics within the framework of both irradiance and temperature, focusing on interactive effects.

Our data from the open ocean strain of *T. pseudonana* indicate that cellular carbon content is not simply a consequence of cell size or growth rate. In the open ocean strain, the combination of supra optimal temperatures (Table 2) and irradiance extremes drastically alters the relationship between cellular carbon content and size; whereas at optimal and suboptimal temperatures, no discernable trend in POC per cell was visible, and neither temperature or irradiance show a consistent effect (Figure 11). D'Souza (2020\*) also found

cellular carbon content to be both independent of cell size, and highest in treatments grown under suboptimal irradiance and high temperature, supporting our findings, but he did not observe any relationship between cell size and temperature. Increasing temperatures have been previously linked to decreasing cell volumes in diatoms grown at one low ( $50 \mu\text{mol photons m}^{-2} \text{s}^{-1}$ ) irradiance (Montagnes & Franklin, 2001), but no additional irradiance regimes were explored. Warmer ocean conditions have been tied to higher growth rates and lower cellular carbon in Southern Ocean diatoms (Boyd et al., 2016), but again only under one irradiance level ( $50 \mu\text{mol photons m}^{-2} \text{s}^{-1}$ ). The interactive effect between temperature and light on the size and carbon content of cells that we observed, has to our knowledge, not been observed before.

When creating models, scientist can utilize a mathematical equation to relate metabolic process to organism size. However, when temperatures and irradiances outside of the optimal are used, these changes can potentially shift the relationship between maximum metabolic rates and size (Finkel et al., 2010). There are also strategies linked to cell size, for instance larger cells can have lower susceptibility to photoinactivation, and therefore incur smaller costs to endure short-term exposures to high light (Key et al., 2010), while being small is often beneficial in a light-limiting environment as internal shading is reduced (Finkel et al., 2010).

While the relationship between cellular carbon content, cell size and environmental drivers appears to adhere to an underlying pattern, is quite complex. The lowest carbon per cell values ( $\sim 50 \text{ pg}$ ) for the open ocean strain are linked to intermediate growth rates ( $1 \text{ day}^{-1}$ ) whereas elevated cellular carbon content ( $\sim 100\text{-}150 \text{ pg}$ ) are seen at both high and low growth rates ( $2.0$  and  $0.5 \text{ day}^{-1}$ ) and maximum values ( $\leq 400 \text{ pg}$ ) at low growth rates, driven



by irradiance (Figure 12). We hypothesize that low irradiances result in low growth rates, which could lead to carbon acquisition without cell division and explain the high amounts of carbon per cell. However, as growth rates increase perhaps there is less carbon build up before cell division causing the cellular carbon value to decrease. Once the combination of optimal temperatures and saturating light is reached, the POC/cell value begins to climb once more. This alludes to the predictability of a relationship between growth rate and cellular carbon, but with the caveat of complex temperature and irradiance interactions dictating the variability.

The relationship between cellular carbon (Y) and growth rates (X) of the coastal strain can be described by a power law relationship ( $Y=4E^{-5} X^{-1.057}$ ,  $R^2=0.4631$ ,  $n=32$ ), between growth rates of 0.37 and 1.55 day<sup>-1</sup> and cellular carbon content of 17.4 pg to 123.0 pg. As with the open ocean strain, lower growth rates appear to result in a higher carbon content, whereas higher growth rates produce a lower amount of carbon per cell. It is also worth noting, that once again cells with low growth rates and high carbon content were often the product of cultures grown at lower irradiances (Figure 12). Since the ranges of temperatures and irradiances tested for this coastal strain were not as broad as those for its open ocean counterpart, this relationship, while cleaner in appearance may only represent a truncated portion of this dynamic.

## 5. Conclusions

The design of this set of experiments is relatively simplistic. We explored a short time frame with a single diatom species, while manipulating only two of the many drivers of growth. While this aids in discovering specific mechanistic understanding of how this

particular species of diatom is influenced by changes in temperature and irradiance it does nothing to provide any insight on community shifts, or answer temporal questions regarding the effects of temperature pulses or fluctuations in light (Stone & Mississippi, 2011). Nevertheless, we have illustrated the high variability in cellular characteristics and photophysical capabilities of these two strains through the concomitant change of just two abiotic parameters. Furthermore, we have identified key points in the range of temperature and irradiance where both drivers influence the response, as well as conditions where one driver has more of an effect than the other. And on top of that we have shown that two strains of the exact same species do not necessarily respond the same way. This experiment illustrates that caution and specificity must be used in the interpretation of performance curves. Simply based on growth rates one would select an entirely different set of temperature and light parameters as “optimal” than if one was interested in maximizing quantum yield or cellular carbon content.

The 1978 launch of the Nimbus-7 satellite which carried the Coastal Zone Color Scanner (CZCS) began the current practice of taking optical measurements of the oceans from space (Smith, 1981). This powerful tool enables researchers to obtain values for Chl *a* on a global scale that would be impractical to attempt from research vessels. The so derived chlorophyll concentration is commonly used to estimate primary productivity, which is used to estimate marine productivity. As shown in this present study and others discussed above, the Chl *a* values obtained from phytoplankton are susceptible to increases and decreases based on environmental conditions and do not always line up with biomass. Possible phytoplankton physiological responses may be to increase their light-harvesting pigment to match the rate of downstream thermal reactions (Finkel et al., 2010). Chlorophyll

measurements thus only tell part of the story, equally important are taxonomy to determine what is there, and physiology to establish how healthy they are (Doney, 2006). To this list, one might also add that it would be helpful to define the abiotic conditions that are producing the Chl *a* value.

Greatly oversimplifying the forecast for our oceans, the diatoms of the future will potentially experience higher temperatures, and because of the stratification caused by those temperature changes, they will also spend more time either suspended in the light or trapped in the dark. Our results illustrate both the well-known response of Chl *a* content to varying light conditions, and a dramatic split in cell size and cellular carbon that occurs in the open ocean strain at supra optimal temperatures (Figure 11). This juxtaposition could potentially create very different Chl *a* to biomass connections, food webs, and carbon export, and hypothetical outcomes could be missed if only values obtained under optimal conditions are used for prediction. The “choices” and energy trade-offs employed by this species of diatom under various combinations of irradiance and temperature make it prudent to have a clear understanding of the mechanisms driving the changes before they are incorporated into sophisticated models. Especially as parameter ranges are pushed outside of the optimal. Moreover, while the potentially predictable relationship between growth rate and cellular carbon content as functions of irradiance and temperature (Figure 12) is promising in providing insight into future food webs, nutrient cycling and carbon export; the complexities and overlapping interactions driving the range warrant further investigations.

## 5. REFERENCES

- Armbrust, E. V., Berges, J. A., Bowler, C., Green, B. R., Martinez, D., Putnam, N. H., Zhou, S. G., Allen, A. E., Apt, K. E., Bechner, M., Brzezinski, M. A., Chaal, B. K., Chiovitti, A., Davis, A. K., Demarest, M. S., Detter, J. C., Glavina, T., Goodstein, D., Hadi, M. Z., Hellsten, U., Hildebrand, M., Jenkins, B. D., Jurka, J., Kapitonov, V. V., Kroger, N., Lau, W. W. Y., Lane, T. W., Larimer, F. W., Lippmeier, J. C., Lucas, S., Medina, M., Montsant, A., Obornik, M., Parker, M. S., Palenik, B., Pazour, G. J., Richardson, P. M., Rynearson, T. A., Saito, M. A., Schwartz, D. C., Thamatrakoln, K., Valentin, K., Vardi, A., Wilkerson, F. P., & Rokhsar, D. S. (2004, Oct). The genome of the diatom *Thalassiosira pseudonana*: Ecology, evolution, and metabolism [Article]. *Science*, 306(5693), 79-86. <https://doi.org/10.1126/science.1101156>
- Asada, K., Kiso, K., & Yoshikawa, K. (1974, Apr 10). Univalent reduction of molecular oxygen by spinach chloroplasts on illumination. *J Biol Chem*, 249(7), 2175-2181.
- Baker, K. G., Robinson, C. M., Radford, D. T., McInnes, A. S., Evenhuis, C., & Doblin, M. A. (2016). Thermal Performance Curves of Functional Traits Aid Understanding of Thermally Induced Changes in Diatom-Mediated Biogeochemical Fluxes [Article]. *Frontiers in Marine Science*, 3, 14, Article Unsp 44. <https://doi.org/10.3389/fmars.2016.00044>
- Barton, A. D., Irwin, A. J., Finkel, Z. V., & Stock, C. A. (2016, Mar). Anthropogenic climate change drives shift and shuffle in North Atlantic phytoplankton communities [Article]. *Proceedings of the National Academy of Sciences of the United States of America*, 113(11), 2964-2969. <https://doi.org/10.1073/pnas.1519080113>
- Behrenfeld, M. J., O'Malley, R. T., Boss, E. S., Westberry, T. K., Graff, J. R., Halsey, K. H., Milligan, A. J., Siegel, D. A., & Brown, M. B. (2016, Mar). Revaluating ocean warming impacts on global phytoplankton [Article]. *Nature Climate Change*, 6(3), 323-330. <https://doi.org/10.1038/nclimate2838>
- Behrenfeld, M. J., O'Malley, R. T., Siegel, D. A., McClain, C. R., Sarmiento, J. L., Feldman, G. C., Milligan, A. J., Falkowski, P. G., Letelier, R. M., & Boss, E. S. (2006, Dec). Climate-driven trends in contemporary ocean productivity [Article]. *Nature*, 444(7120), 752-755. <https://doi.org/10.1038/nature05317>
- Berges, J. A., Varela, D. E., & Harrison, P. J. (2002). Effects of temperature on growth rate, cell composition and nitrogen metabolism in the marine diatom *Thalassiosira pseudonana* (Bacillariophyceae) [Article]. *Marine Ecology Progress Series*, 225, 139-146. <https://doi.org/10.3354/meps225139>

- Bojko, M., Brzostowska, K., Kuczynska, P., Latowski, D., Olchawa-Pajor, M., Krzeszowiec, W., Waloszek, A., & Strzalka, K. (2013). Temperature effect on growth, and selected parameters of *Phaeodactylum tricornutum* in batch cultures. *Acta Biochimica Polonica*, *60*(4), 861-864. <Go to ISI>://WOS:000329557400062
- Bopp, L., Resplandy, L., Orr, J. C., Doney, S. C., Dunne, J. P., Gehlen, M., Halloran, P., Heinze, C., Ilyina, T., Seferian, R., Tjiputra, J., & Vichi, M. (2013). Multiple stressors of ocean ecosystems in the 21st century: projections with CMIP5 models [Article]. *Biogeosciences*, *10*(10), 6225-6245. <https://doi.org/10.5194/bg-10-6225-2013>
- Boyd, P. W., Collins, S., Dupont, S., Fabricius, K., Gattuso, J. P., Havenhand, J., Hutchins, D. A., Riebesell, U., Rintoul, M. S., Vichi, M., Biswas, H., Ciotti, A., Gao, K., Gehlen, M., Hurd, C. L., Kurihara, H., McGraw, C. M., Navarro, J. M., Nilsson, G. E., Passow, U., & Portner, H. O. (2018, Jun). Experimental strategies to assess the biological ramifications of multiple drivers of global ocean change-A review [Review]. *Global Change Biology*, *24*(6), 2239-2261. <https://doi.org/10.1111/gcb.14102>
- Boyd, P. W., Dillingham, P. W., McGraw, C. M., Armstrong, E. A., Cornwall, C. E., Feng, Y. Y., Hurd, C. L., Gault-Ringold, M., Roleda, M. Y., Timmins-Schiffman, E., & Nunn, B. L. (2016, Feb). Physiological responses of a Southern Ocean diatom to complex future ocean conditions [Article]. *Nature Climate Change*, *6*(2), 207-+. <https://doi.org/10.1038/nclimate2811>
- Boyd, P. W., Doney, S. C., Strzepek, R., Dusenberry, J., Lindsay, K., & Fung, I. (2008). Climate-mediated changes to mixed-layer properties in the Southern Ocean: assessing the phytoplankton response [Review]. *Biogeosciences*, *5*(3), 847-864. <https://doi.org/10.5194/bg-5-847-2008>
- Boyd, P. W., Rynearson, T. A., Armstrong, E. A., Fu, F. X., Hayashi, K., Hu, Z. X., Hutchins, D. A., Kudela, R. M., Litchman, E., Mulholland, M. R., Passow, U., Strzepek, R. F., Whittaker, K. A., Yu, E., & Thomas, M. K. (2013, May). Marine Phytoplankton Temperature versus Growth Responses from Polar to Tropical Waters - Outcome of a Scientific Community-Wide Study [Article]. *Plos One*, *8*(5), 17, Article e63091. <https://doi.org/10.1371/journal.pone.0063091>
- Breitbart, D. L., Salisbury, J., Bernhard, J. M., Cai, W. J., Dupont, S., Doney, S. C., Kroeker, K. J., Levin, L. A., Long, W. C., Milke, L. M., Miller, S. H., Phelan, B., Passow, U., Seibel, B. A., Todgham, A. E., & Tarrant, A. M. (2015, Jun). And on Top of All That... Coping with Ocean Acidification in the Midst of Many Stressors [Article]. *Oceanography*, *28*(2), 48-61. <https://doi.org/10.5670/oceanog.2015.31>
- Bretherton, L., Williams, A., Genzer, J., Hillhouse, J., Kamalanathan, M., Finkel, Z. V., & Quigg, A. (2018, Jun). PHYSIOLOGICAL RESPONSE OF 10 PHYTOPLANKTON SPECIES EXPOSED TO MACONDO OIL AND THE DISPERSANT, COREXIT [Article]. *Journal of Phycology*, *54*(3), 317-328. <https://doi.org/10.1111/jpy.12625>

- Brown, J. H., Gillooly, J. F., Allen, A. P., Savage, V. M., & West, G. B. (2004, Jul). Toward a metabolic theory of ecology [Review]. *Ecology*, 85(7), 1771-1789. <https://doi.org/10.1890/03-9000>
- Clayton, T. D., & Byrne, R. H. (1993, Oct). SPECTROPHOTOMETRIC SEAWATER PH MEASUREMENTS - TOTAL HYDROGEN-ION CONCENTRATION SCALE CALIBRATION OF M-CRESOL PURPLE AND AT-SEA RESULTS [Article]. *Deep-Sea Research Part I-Oceanographic Research Papers*, 40(10), 2115-2129. [https://doi.org/10.1016/0967-0637\(93\)90048-8](https://doi.org/10.1016/0967-0637(93)90048-8)
- Consalvey, M., Perkins, R. G., Paterson, D. M., & Underwood, G. J. C. (2005, May). Pam fluorescence: A beginners guide for benthic diatomists [Article]. *Diatom Research*, 20(1), 1-22. <Go to ISI>://WOS:000228697800001
- D'Souza, N., Laws, E. A., & Passow, U. (2020\*). Growth and Productivity Response of a diatom to Multiple Stressors. \*In revision for submission to *Journal of Phycology*.
- Dickson, A. G., Sabine, C. L., & Christian, J. R. E. (2007). *Guide to Best Practices for Ocean CO2 Measurements*.
- Doney, S. C. (2006, Dec). Oceanography - Plankton in a warmer world [Editorial Material]. *Nature*, 444(7120), 695-696. <https://doi.org/10.1038/444695a>
- Doney, S. C., Fabry, V. J., Feely, R. A., & Kleypas, J. A. (2009). Ocean Acidification: The Other CO2 Problem. In *Annual Review of Marine Science* (Vol. 1, pp. 169-192). Annual Reviews. <https://doi.org/10.1146/annurev.marine.010908.163834>
- Doney, S. C., Ruckelshaus, M., Duffy, J. E., Barry, J. P., Chan, F., English, C. A., Galindo, H. M., Grebmeier, J. M., Hollowed, A. B., Knowlton, N., Polovina, J., Rabalais, N. N., Sydeman, W. J., & Talley, L. D. (2012). Climate Change Impacts on Marine Ecosystems. In C. A. Carlson & S. J. Giovannoni (Eds.), *Annual Review of Marine Science, Vol 4* (Vol. 4, pp. 11-37). Annual Reviews. <https://doi.org/10.1146/annurev-marine-041911-111611>
- Dubinsky, Z., & Stambler, N. (2009, 09/03). Photoacclimation processes in phytoplankton: mechanisms, consequences, and applications. *Aquatic Microbial Ecology*, 56, 163-176. <https://doi.org/10.3354/ame01345>
- Eppley, R. W. (1972). TEMPERATURE AND PHYTOPLANKTON GROWTH IN SEA [Review]. *Fishery Bulletin*, 70(4), 1063-1085. <Go to ISI>://WOS:A1972O454900001

- Falkowski, P. G., & Owens, T. G. (1980). LIGHT-SHADE ADAPTATION - 2 STRATEGIES IN MARINE-PHYTOPLANKTON [Article]. *Plant Physiology*, 66(4), 592-595. <https://doi.org/10.1104/pp.66.4.592>
- Falkowski, P. G., Owens, T. G., Ley, A. C., & Mauzerall, D. C. (1981). EFFECTS OF GROWTH IRRADIANCE LEVELS ON THE RATIO OF REACTION CENTERS IN 2 SPECIES OF MARINE-PHYTOPLANKTON [Article]. *Plant Physiology*, 68(4), 969-973. <https://doi.org/10.1104/pp.68.4.969>
- Falkowski, P. G., & Raven, J. A. (1997). *Aquatic photosynthesis*. Blackwell Science.
- Fangue, N. A., O'Donnell, M. J., Sewell, M. A., Matson, P. G., MacPherson, A. C., & Hofmann, G. E. (2010, Aug). A laboratory-based, experimental system for the study of ocean acidification effects on marine invertebrate larvae [Article]. *Limnology and Oceanography-Methods*, 8, 441-452. <https://doi.org/10.4319/lom.2010.8.441>
- Feng, Y. Y., Hare, C. E., Leblanc, K., Rose, J. M., Zhang, Y. H., DiTullio, G. R., Lee, P. A., Wilhelm, S. W., Rowe, J. M., Sun, J., Nemcek, N., Gueguen, C., Passow, U., Benner, I., Brown, C., & Hutchins, D. A. (2009). Effects of increased pCO<sub>2</sub> and temperature on the North Atlantic spring bloom. I. The phytoplankton community and biogeochemical response [Article]. *Marine Ecology Progress Series*, 388, 13-25. <https://doi.org/10.3354/meps08133>
- Finkel, Z. V., Beardall, J., Flynn, K. J., Quigg, A., Rees, T. A. V., & Raven, J. A. (2010, Jan). Phytoplankton in a changing world: cell size and elemental stoichiometry [Review]. *Journal of Plankton Research*, 32(1), 119-137. <https://doi.org/10.1093/plankt/fbp098>
- Gao, K. S., Beardall, J., Hader, D. P., Hall-Spencero, J. M., Gao, G., & Hutchins, D. A. (2019, Jun). Effects of Ocean Acidification on Marine Photosynthetic Organisms Under the Concurrent Influences of Warming, UV Radiation, and Deoxygenation [Review]. *Frontiers in Marine Science*, 6, 18, Article Unsp 322. <https://doi.org/10.3389/fmars.2019.00322>
- Gao, K. S., Helbling, E. W., Hader, D. P., & Hutchins, D. A. (2012). Responses of marine primary producers to interactions between ocean acidification, solar radiation, and warming [Article]. *Marine Ecology Progress Series*, 470, 167-189. <https://doi.org/10.3354/meps10043>
- Gao, K. S., Xu, J. T., Gao, G., Li, Y. H., Hutchins, D. A., Huang, B. Q., Wang, L., Zheng, Y., Jin, P., Cai, X. N., Hader, D. P., Li, W., Xu, K., Liu, N. N., & Riebesell, U. (2012, Jul). Rising CO<sub>2</sub> and increased light exposure synergistically reduce marine primary productivity [Article]. *Nature Climate Change*, 2(7), 519-523. <https://doi.org/10.1038/nclimate1507>

- Gechev, T. S., Van Breusegem, F., Stone, J. M., Denev, I., & Laloi, C. (2006, Nov). Reactive oxygen species as signals that modulate plant stress responses and programmed cell death. *Bioessays*, 28(11), 1091-1101. <https://doi.org/10.1002/bies.20493>
- Geider, R. J., MacIntyre, H. L., & Kana, T. M. (1997, Mar). Dynamic model of phytoplankton growth and acclimation: Responses of the balanced growth rate and the chlorophyll a:carbon ratio to light, nutrient-limitation and temperature [Article]. *Marine Ecology Progress Series*, 148(1-3), 187-200. <https://doi.org/10.3354/meps148187>
- Gittings, J. A., Raitsos, D. E., Krokos, G., & Hoteit, I. (2018, 2018/02/02). Impacts of warming on phytoplankton abundance and phenology in a typical tropical marine ecosystem. *Scientific Reports*, 8(1), 2240. <https://doi.org/10.1038/s41598-018-20560-5>
- Goto, N., Kihira, M., & Ishida, N. (2008, Oct). Seasonal distribution of photosynthetically active phytoplankton using pulse amplitude modulated fluorometry in the large monomictic Lake Biwa, Japan [Article]. *Journal of Plankton Research*, 30(10), 1169-1177. <https://doi.org/10.1093/plankt/fbn073>
- Gruber, N., Clement, D., Carter, B. R., Feely, R. A., van Heuven, S., Hoppema, M., Ishii, M., Key, R. M., Kozyr, A., Lauvset, S. K., Lo Monaco, C., Mathis, J. T., Murata, A., Olsen, A., Perez, F. F., Sabine, C. L., Tanhua, T., & Wanninkhof, R. (2019, Mar). The oceanic sink for anthropogenic CO<sub>2</sub> from 1994 to 2007 [Article]. *Science*, 363(6432), 1193-+. <https://doi.org/10.1126/science.aau5153>
- Guillard, R. R. L. (1975). Culture of Phytoplankton for Feeding Marine Invertebrates. In W. L. Smith & M. H. Chanley (Eds.), *Culture of Marine Invertebrate Animals: Proceedings — 1st Conference on Culture of Marine Invertebrate Animals Greenport* (pp. 29-60). Springer US. [https://doi.org/10.1007/978-1-4615-8714-9\\_3](https://doi.org/10.1007/978-1-4615-8714-9_3)
- Gunderson, A. R., Armstrong, E. J., & Stillman, J. H. (2016). Multiple Stressors in a Changing World: The Need for an Improved Perspective on Physiological Responses to the Dynamic Marine Environment. *Annual Review of Marine Science*, Vol 8, 8, 357-+. <https://doi.org/10.1146/annurev-marine-122414-033953>
- Hader, D. P., & Gao, K. S. (2015). Interactions of anthropogenic stress factors on marine phytoplankton [Review]. *Frontiers in Environmental Science*, 3, 14, Article 14. <https://doi.org/10.3389/fenvs.2015.00014>
- Hare, C. E., Leblanc, K., DiTullio, G. R., Kudela, R. M., Zhang, Y., Lee, P. A., Riseman, S., & Hutchins, D. A. (2007). Consequences of increased temperature and CO<sub>2</sub> for phytoplankton community structure in the Bering Sea [Article]. *Marine Ecology Progress Series*, 352, 9-16. <https://doi.org/10.3354/meps07182>



- Helbling, E. W., Buma, A. G. J., Boelen, P., van der Strate, H. J., Giordanino, M. V. F., & Villafane, V. E. (2011, Jul). Increase in Rubisco activity and gene expression due to elevated temperature partially counteracts ultraviolet radiation-induced photoinhibition in the marine diatom *Thalassiosira weissflogii* [Article]. *Limnology and Oceanography*, *56*(4), 1330-1342. <https://doi.org/10.4319/lo.2011.56.4.1330>
- Henson, S. A., Beaulieu, C., Ilyina, T., John, J. G., Long, M., Seferian, R., Tjiputra, J., & Sarmiento, J. L. (2017, Mar). Rapid emergence of climate change in environmental drivers of marine ecosystems. *Nature Communications*, *8*, Article 14682. <https://doi.org/10.1038/ncomms14682>
- Hutchins, D. A., & Fu, F. X. (2017, Jun). Microorganisms and ocean global change [Review]. *Nature Microbiology*, *2*(6), 11, Article 17058. <https://doi.org/10.1038/nmicrobiol.2017.58>
- Jakob, T., Wagner, H., Stehfest, K., & Wilhelm, C. (2007). A complete energy balance from photons to new biomass reveals a light- and nutrient-dependent variability in the metabolic costs of carbon assimilation [Article]. *Journal of Experimental Botany*, *58*(8), 2101-2112. <https://doi.org/10.1093/jxb/erm084>
- Janknegt, P. J., De Graaff, C. M., Van De Poll, W. H., Visser, R. J. W., Rijstenbil, J. W., & Buma, A. G. J. (2009, 2009/11/01). Short-term antioxidative responses of 15 microalgae exposed to excessive irradiance including ultraviolet radiation. *European Journal of Phycology*, *44*(4), 525-539. <https://doi.org/10.1080/09670260902943273>
- Kester, D. R., Duedall, I. W., Connors, D. N., & Pytkowicz, R. M. (1967). PREPARATION OF ARTIFICIAL SEAWATER [Note]. *Limnology and Oceanography*, *12*(1), 176-+. <https://doi.org/10.4319/lo.1967.12.1.0176>
- Key, T., McCarthy, A., Campbell, D. A., Six, C., Roy, S., & Finkel, Z. V. (2010, Jan). Cell size trade-offs govern light exploitation strategies in marine phytoplankton [Article]. *Environmental Microbiology*, *12*(1), 95-104. <https://doi.org/10.1111/j.1462-2920.2009.02046.x>
- Kreyling, J., Schweiger, A. H., Bahn, M., Ineson, P., Migliavacca, M., Morel-Journel, T., Christiansen, J. R., Schtickzelle, N., & Larsen, K. S. (2018, Nov). To replicate, or not to replicate - that is the question: how to tackle nonlinear responses in ecological experiments [Article]. *Ecology Letters*, *21*(11), 1629-1638. <https://doi.org/10.1111/ele.13134>
- Kromkamp, J., & Peene, J. (1999, 1999/03/01). Estimation of phytoplankton photosynthesis and nutrient limitation in the Eastern Scheldt estuary using variable fluorescence. *Aquatic Ecology*, *33*(1), 101-104. <https://doi.org/10.1023/A:1009900124650>

- Lakeman, M., Von Dassow, P., & Cattolico, R. A. (2009, 06/01). The strain concept in phytoplankton ecology. *Harmful Algae*, 8, 746-758. <https://doi.org/10.1016/j.hal.2008.11.011>
- Lassen, M. K., Nielsen, K. D., Richardson, K., Garde, K., & Schluter, L. (2010, Jan). The effects of temperature increases on a temperate phytoplankton community - A mesocosm climate change scenario [Article]. *Journal of Experimental Marine Biology and Ecology*, 383(1), 79-88. <https://doi.org/10.1016/j.jembe.2009.10.014>
- Lavaud, J., Strzepek, R. F., & Kroth, P. G. (2007, May). Photoprotection capacity differs among diatoms: Possible consequences on the spatial distribution of diatoms related to fluctuations in the underwater light climate [Article]. *Limnology and Oceanography*, 52(3), 1188-1194. <https://doi.org/10.4319/lo.2007.52.3.1188>
- Laws, E. A., McClellan, S. A., & Passow, U. (2020, 2020/08/04). Interactive Effects of CO<sub>2</sub>, Temperature, Irradiance, and Nutrient Limitation on the Growth and Physiology of the Marine Diatom *Thalassiosira pseudonana* (Coscinodiscophyceae). *Journal of Phycology*, n/a(n/a). <https://doi.org/10.1111/jpy.13048>
- Li, G., & Campbell, D. A. (2013, Jan). Rising CO<sub>2</sub> Interacts with Growth Light and Growth Rate to Alter Photosystem II Photoinactivation of the Coastal Diatom *Thalassiosira pseudonana* [Article]. *Plos One*, 8(1), 13, Article e55562. <https://doi.org/10.1371/journal.pone.0055562>
- Lindsey, R., Scott, M., & Simmon, R. (2010, 2020-03-31). *What are Phytoplankton?*  
<https://earthobservatory.nasa.gov/contact/>.  
<https://earthobservatory.nasa.gov/features/Phytoplankton>
- Liu, R., Ran, X. F., Bai, F., Xu, J. Z., Yang, S. Q., Shi, J. Q., & Wu, Z. X. (2015). Use of chlorophyll a fluorescence to elucidate the toxicity target of N-phenyl-2-naphthylamine on photosynthetic system of *Cylindrospermopsis raciborskii* (Cyanobacteria) [Article]. *Phycologia*, 54(1), 12-19. <https://doi.org/10.2216/14-050.1>
- Long, S. P., Humphries, S., & Falkowski, P. G. (1994). PHOTONHIBITION OF PHOTOSYNTHESIS IN NATURE [Review]. *Annual Review of Plant Physiology and Plant Molecular Biology*, 45, 633-662. <https://doi.org/10.1146/annurev.pp.45.060194.003221>
- Lopez-Urrutia, A., San Martin, E., Harris, R. P., & Irigoien, X. (2006, Jun). Scaling the metabolic balance of the oceans [Article]. *Proceedings of the National Academy of Sciences of the United States of America*, 103(23), 8739-8744. <https://doi.org/10.1073/pnas.0601137103>

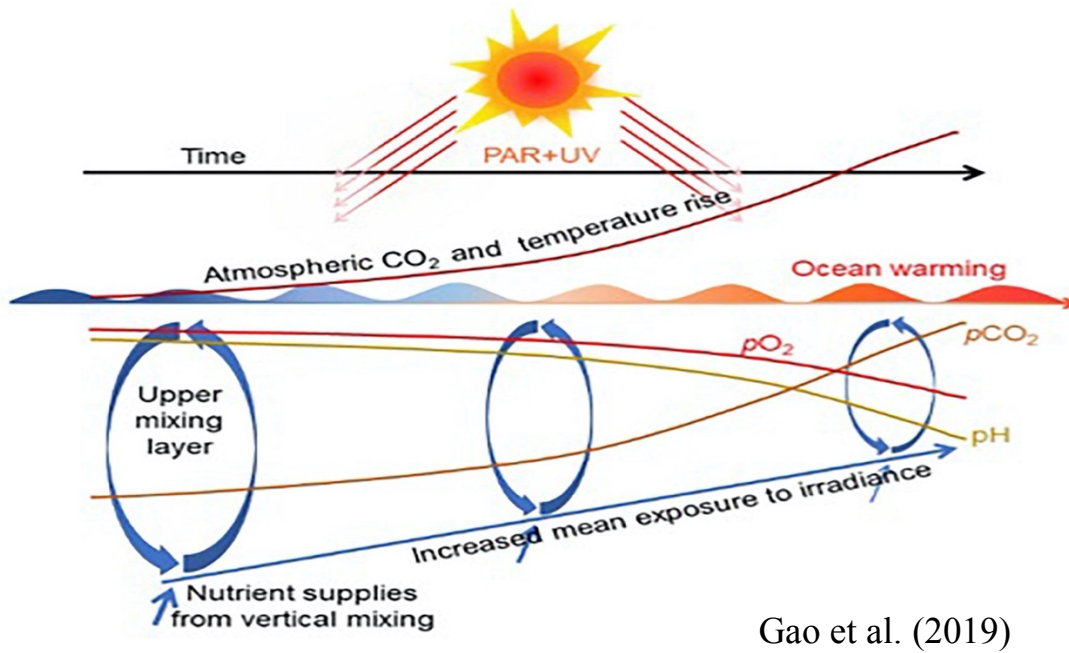
- Mehler, A. H. (1951). Studies on reactions of illuminated chloroplasts. I. Mechanism of the reduction of oxygen and other Hill reagents. *Archives of biochemistry and biophysics*, 33(1), 65-77.  
<https://ezproxyprod.ucs.louisiana.edu:2443/login?url=http://search.ebscohost.com/login.aspx?direct=true&AuthType=ip,cookie,uid,url&db=cmedm&AN=14857775&site=eds-live>
- Montagnes, D. J. S., & Franklin, D. J. (2001, Dec). Effect of temperature on diatom volume, growth rate, and carbon and nitrogen content: Reconsidering some paradigms [Article]. *Limnology and Oceanography*, 46(8), 2008-2018. <https://doi.org/10.4319/lo.2001.46.8.2008>
- Nelson, D. M., Treguer, P., Brzezinski, M. A., Leynaert, A., & Queguiner, B. (1995, Sep). PRODUCTION AND DISSOLUTION OF BIOGENIC SILICA IN THE OCEAN - REVISED GLOBAL ESTIMATES, COMPARISON WITH REGIONAL DATA AND RELATIONSHIP TO BIOGENIC SEDIMENTATION [Review]. *Global Biogeochemical Cycles*, 9(3), 359-372.  
<https://doi.org/10.1029/95gb01070>
- Passow, U. (2012, Jan 20). The abiotic formation of TEP under different ocean acidification scenarios. *Marine Chemistry*, 128, 72-80. <https://doi.org/10.1016/j.marchem.2011.10.004>
- Passow, U., & Laws, E. A. (2015, Dec). Ocean acidification as one of multiple stressors: growth response of *Thalassiosira weissflogii* (diatom) under temperature and light stress [Article]. *Marine Ecology Progress Series*, 541, 75-90. <https://doi.org/10.3354/meps11541>
- Platt, T., & Jassby, A. D. (1976). RELATIONSHIP BETWEEN PHOTOSYNTHESIS AND LIGHT FOR NATURAL ASSEMBLAGES OF COASTAL MARINE-PHYTOPLANKTON [Article]. *Journal of Phycology*, 12(4), 421-430. <https://doi.org/10.1111/j.1529-8817.1976.tb02866.x>
- Regaudie-De-Gioux, A., & Duarte, C. M. (2012, Feb). Temperature dependence of planktonic metabolism in the ocean [Article]. *Global Biogeochemical Cycles*, 26, 10, Article Gb1015.  
<https://doi.org/10.1029/2010gb003907>
- Sarthou, G., Timmermans, K. R., Blain, S., & Treguer, P. (2005, Jan). Growth physiology and fate of diatoms in the ocean: a review [Review]. *Journal of Sea Research*, 53(1-2), 25-42.  
<https://doi.org/10.1016/j.seares.2004.01.007>
- Smith, R. C. (1981). REMOTE-SENSING AND DEPTH DISTRIBUTION OF OCEAN CHLOROPHYLL [Note]. *Marine Ecology Progress Series*, 5(3), 359-361. <https://doi.org/10.3354/meps005359>
- Steele, J. H. (1962). ENVIRONMENTAL CONTROL OF PHOTOSYNTHESIS IN THE SEA [Article]. *Limnology and Oceanography*, 7(2), 137-150. <https://doi.org/10.4319/lo.1962.7.2.0137>

- Stone, M. L., & Mississippi, U. o. S. (2011). *Measuring and Comparing Quantum Yield in Two Species of Marine Diatoms Subjected to Constant and Fluctuating Light Conditions* [Master's Thesis, The University of Southern Mississippi].  
[https://aquila.usm.edu/cgi/viewcontent.cgi?article=1246&context=masters\\_theses](https://aquila.usm.edu/cgi/viewcontent.cgi?article=1246&context=masters_theses)  
[https://aquila.usm.edu/masters\\_theses/221](https://aquila.usm.edu/masters_theses/221)
- Stramski, D., Sciandra, A., & Claustre, H. (2002, Mar). Effects of temperature, nitrogen, and light limitation on the optical properties of the marine diatom *Thalassiosira pseudonana* [Article]. *Limnology and Oceanography*, 47(2), 392-403.  
<https://doi.org/10.4319/lo.2002.47.2.0392>
- Strickland, J. D. H., & Parsons, T. R. (1972). *A practical handbook of seawater analysis*. Fisheries Research Board of Canada.
- Strzepek, R. F., & Harrison, P. J. (2004, Oct). Photosynthetic architecture differs in coastal and oceanic diatoms [Article]. *Nature*, 431(7009), 689-692.  
<https://doi.org/10.1038/nature02954>
- Taucher, J., Jones, J., James, A., Brzezinski, M. A., Carlson, C. A., Riebesell, U., & Passow, U. (2015, May). Combined effects of CO<sub>2</sub> and temperature on carbon uptake and partitioning by the marine diatoms *Thalassiosira weissflogii* and *Dactyliosolen fragilissimus* [Article]. *Limnology and Oceanography*, 60(3), 901-919. <https://doi.org/10.1002/lno.10063>
- Thomas, M. K., Aranguren-Gassis, M., Kremer, C. T., Gould, M. R., Anderson, K., Klausmeier, C. A., & Litchman, E. (2017, Aug). Temperature-nutrient interactions exacerbate sensitivity to warming in phytoplankton [Article]. *Global Change Biology*, 23(8), 3269-3280.  
<https://doi.org/10.1111/gcb.13641>
- Thomas, M. K., Kremer, C. T., Klausmeier, C. A., & Litchman, E. (2012, Nov). A Global Pattern of Thermal Adaptation in Marine Phytoplankton [Article]. *Science*, 338(6110), 1085-1088.  
<https://doi.org/10.1126/science.1224836>
- Todgham, A. E., & Stillman, J. H. (2013, Oct). Physiological Responses to Shifts in Multiple Environmental Stressors: Relevance in a Changing World [Article]. *Integrative and Comparative Biology*, 53(4), 539-544. <https://doi.org/10.1093/icb/ict086>
- Trimborn, S., Hoppe, C. J. M., Taylor, B. B., Bracher, A., & Hassler, C. (2015, Apr). Physiological characteristics of open ocean and coastal phytoplankton communities of Western Antarctic Peninsula and Drake Passage waters [Article]. *Deep-Sea Research Part I-Oceanographic Research Papers*, 98, 115-124. <https://doi.org/10.1016/j.dsr.2014.12.010>

- Trombetta, T., Vidussi, F., Mas, S., Parin, D., Simier, M., & Mostajir, B. (2019). Water temperature drives phytoplankton blooms in coastal waters. *Plos One*, *14*(4), e0214933. <https://doi.org/10.1371/journal.pone.0214933>
- van de Poll, W., van Leeuwe, M., Roggeveld, J., & Buma, A. (2005, 08/01). Nutrient limitation and high irradiance reduce PAR and UV-induced viability loss in the Antarctic diatom *Chaetoceros brevis* (Bacillariophyceae). *Journal of Phycology*, *41*, 840-850. <https://doi.org/10.1111/j.1529-8817.2005.00105.x>
- Wagner, H., Jakob, T., Fanesi, A., & Wilhelm, C. (2017, Sep). Towards an understanding of the molecular regulation of carbon allocation in diatoms: the interaction of energy and carbon allocation [Review]. *Philosophical Transactions of the Royal Society B-Biological Sciences*, *372*(1728), 10, Article 20160410. <https://doi.org/10.1098/rstb.2016.0410>
- Wolf, K. K. E., Romanelli, E., Rost, B., John, U., Collins, S., Weigand, H., & Hoppe, C. J. M. (2019, Sep). Company matters: The presence of other genotypes alters traits and intraspecific selection in an Arctic diatom under climate change. *Global Change Biology*, *25*(9), 2869-2884. <https://doi.org/10.1111/gcb.14675>
- Wong, C. Y., Teoh, M. L., Phang, S. M., Lim, P. E., & Beardall, J. (2015, Oct). Interactive Effects of Temperature and UV Radiation on Photosynthesis of *Chlorella* Strains from Polar, Temperate and Tropical Environments: Differential Impacts on Damage and Repair [Article]. *Plos One*, *10*(10), 14, Article e0139469. <https://doi.org/10.1371/journal.pone.0139469>
- Zhu, S. H., & Green, B. R. (2010, Aug). Photoprotection in the diatom *Thalassiosira pseudonana*: Role of L1818-like proteins in response to high light stress. *Biochimica Et Biophysica Acta-Bioenergetics*, *1797*(8), 1449-1457. <https://doi.org/10.1016/j.bbabi.2010.04.003>

## 6. FIGURES AND TABLES

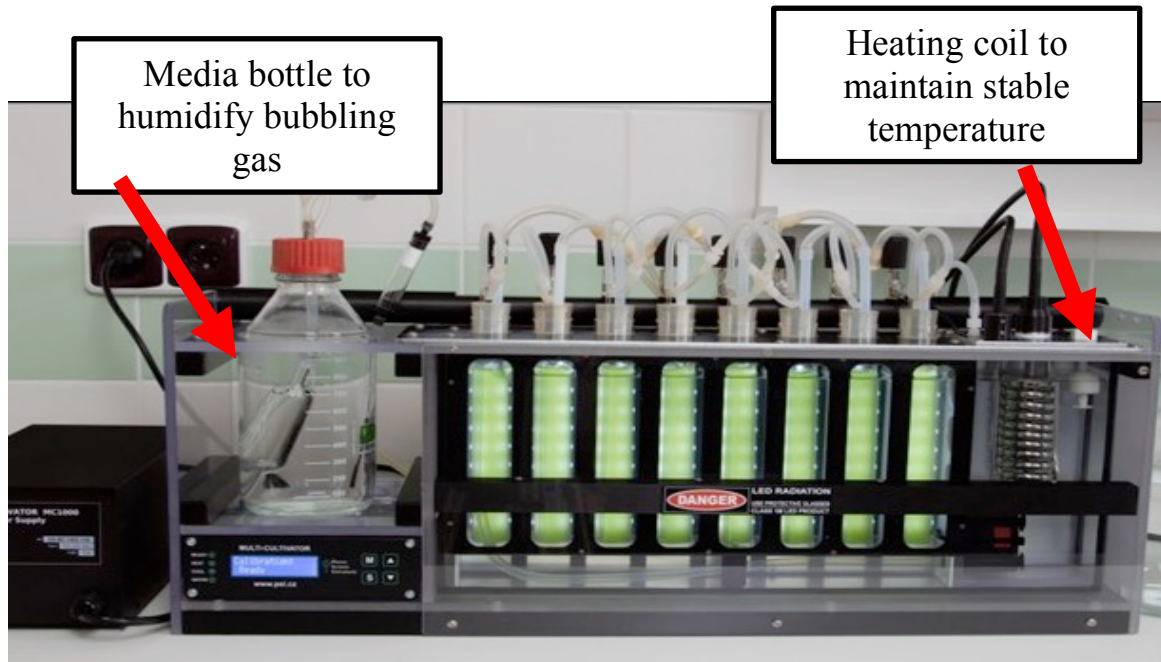
**Figure 1**



Gao et al. (2019)

**Figure 1.** Ocean acidification, warming, and deoxygenation associated with increasing atmospheric CO<sub>2</sub> rise. Shoaling of the upper mixed layer (UML) due to warming exposes organisms dwelling there to higher levels of solar radiation.

**Figure 2**



Multicultivator Z160-OD Photon systems

**Figure 2.** Image of the multicultivator Z160-OD used in these experiments

Figure 3

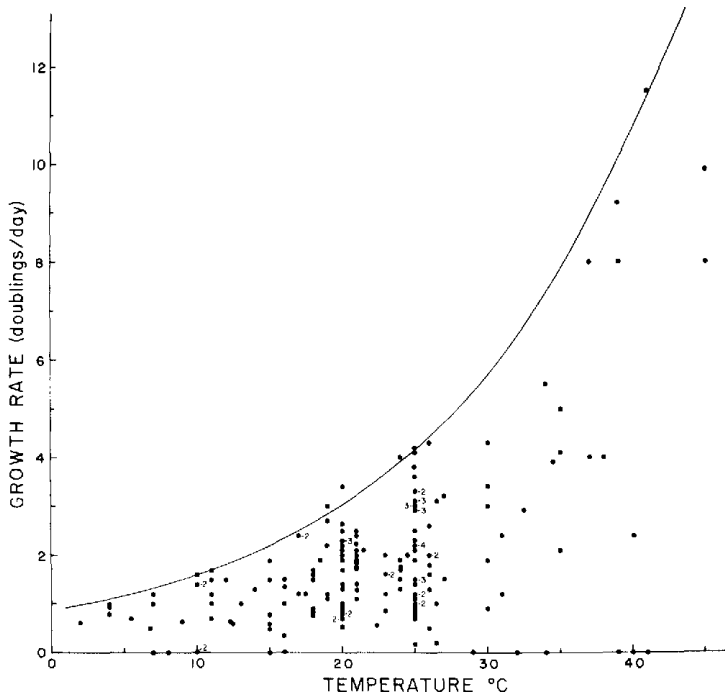


Figure A: Variation in the specific growth rate ( $\mu$ ) of photoautotrophic unicellular algae with temperature.

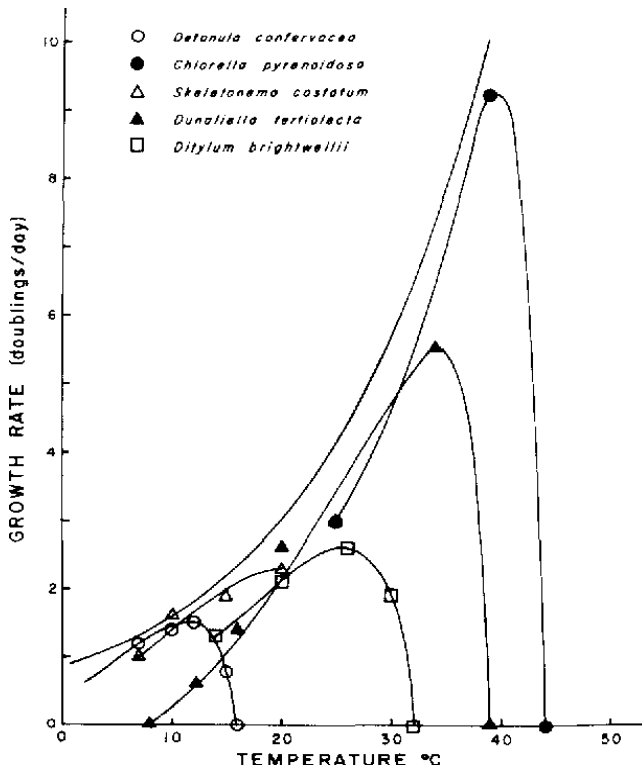
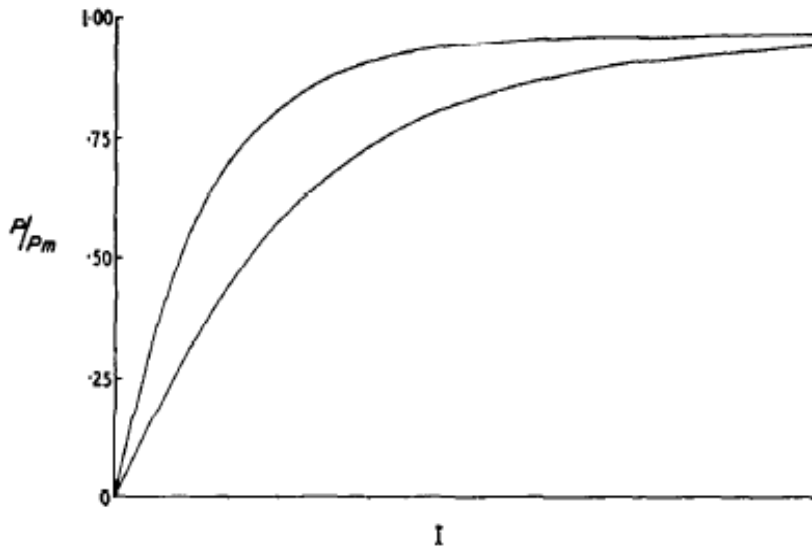


Figure B: Growth rate vs. temperature for five unicellular algae with different temperature optima.

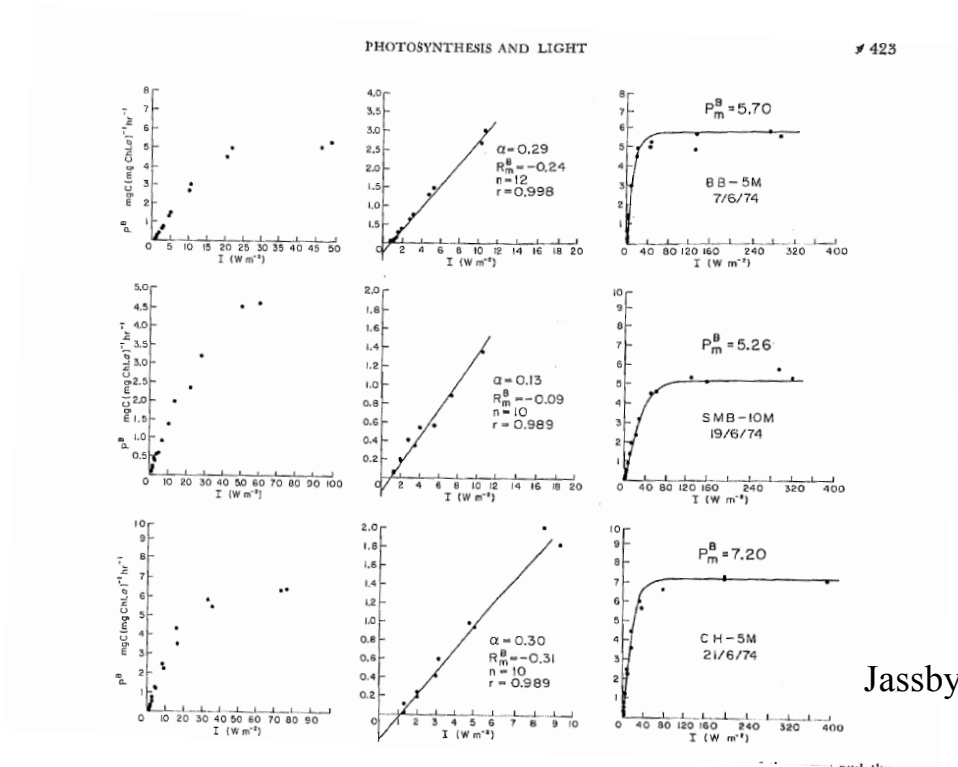
Eppley 1972



Figure 4



Steele 1967



Jassby and Platt 1976

Figure 4. Graphics from Steel 1967 and Jassby and Platt 1976 illustrating typical relationships between photosynthesis and light

**Figure 5A**

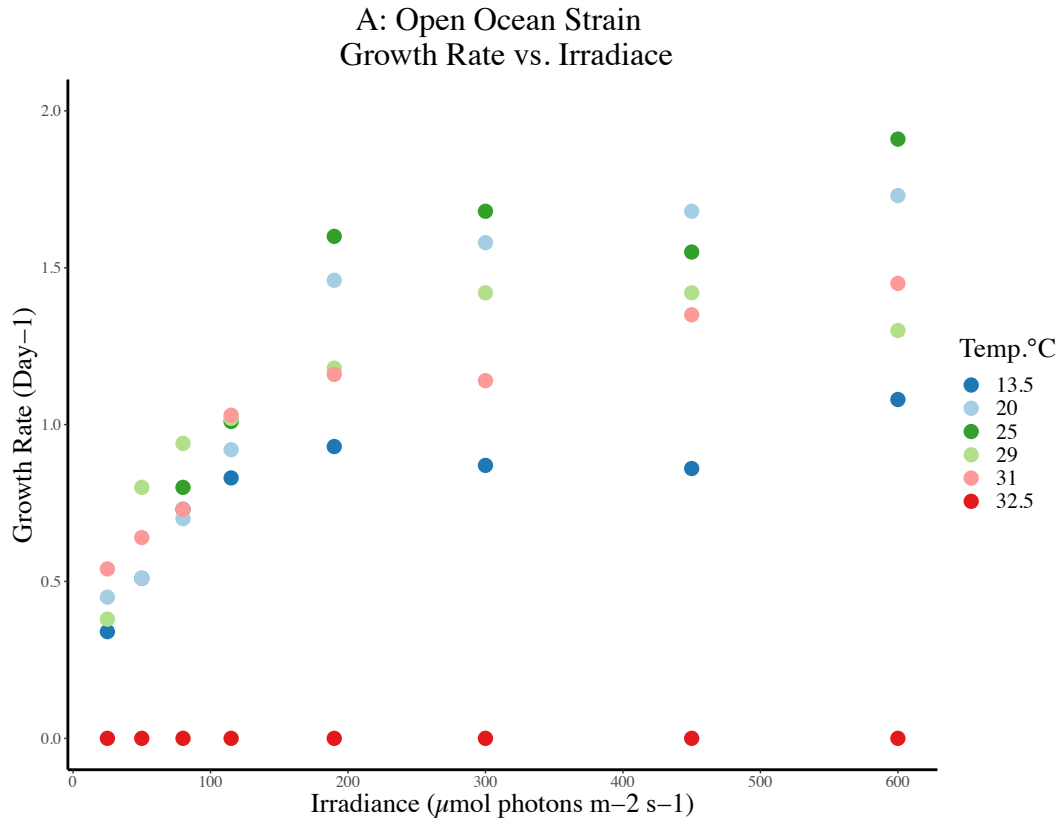


**Figure 5A.** Growth rates for the open ocean strain as they relate to temperature and irradiance.

**Figure 5B**

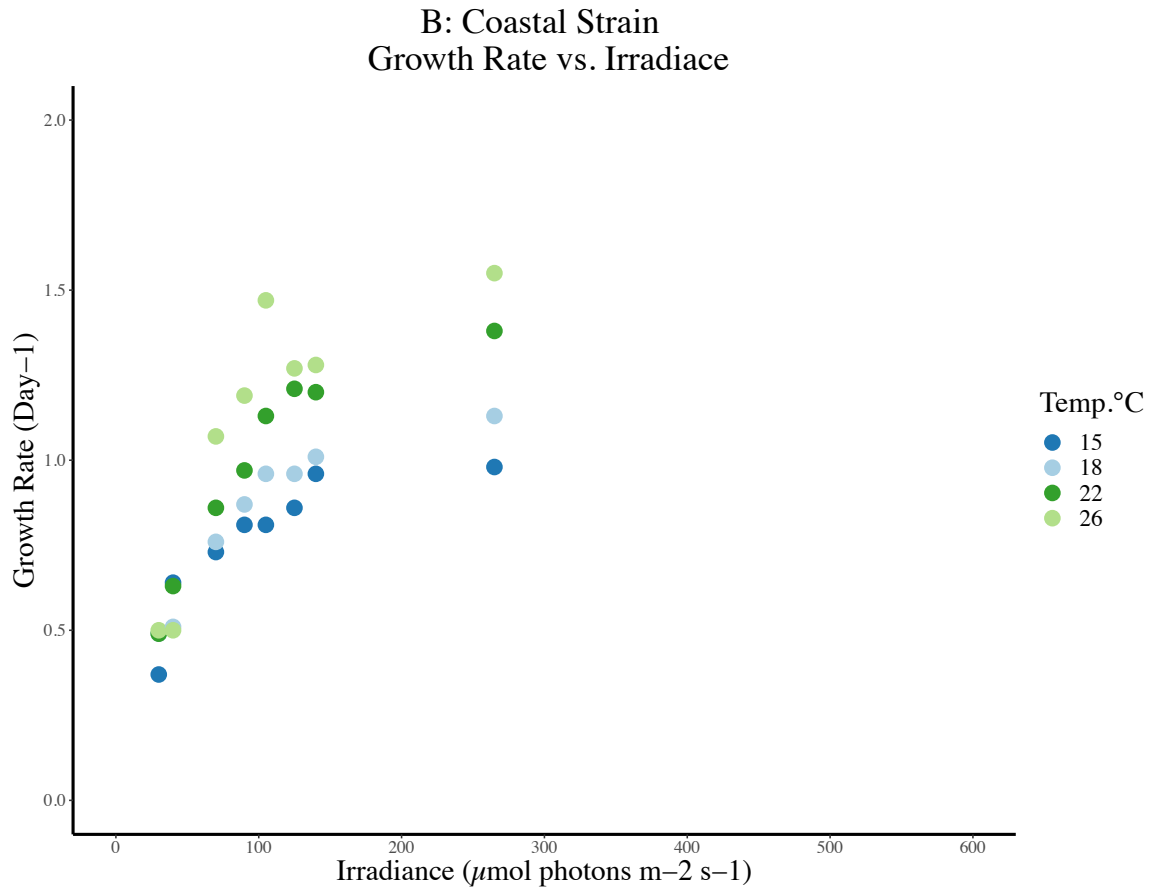


**Figure 5B.** Growth rates for the coastal strain as they relate to temperature and irradiance.

**Figure 5C**

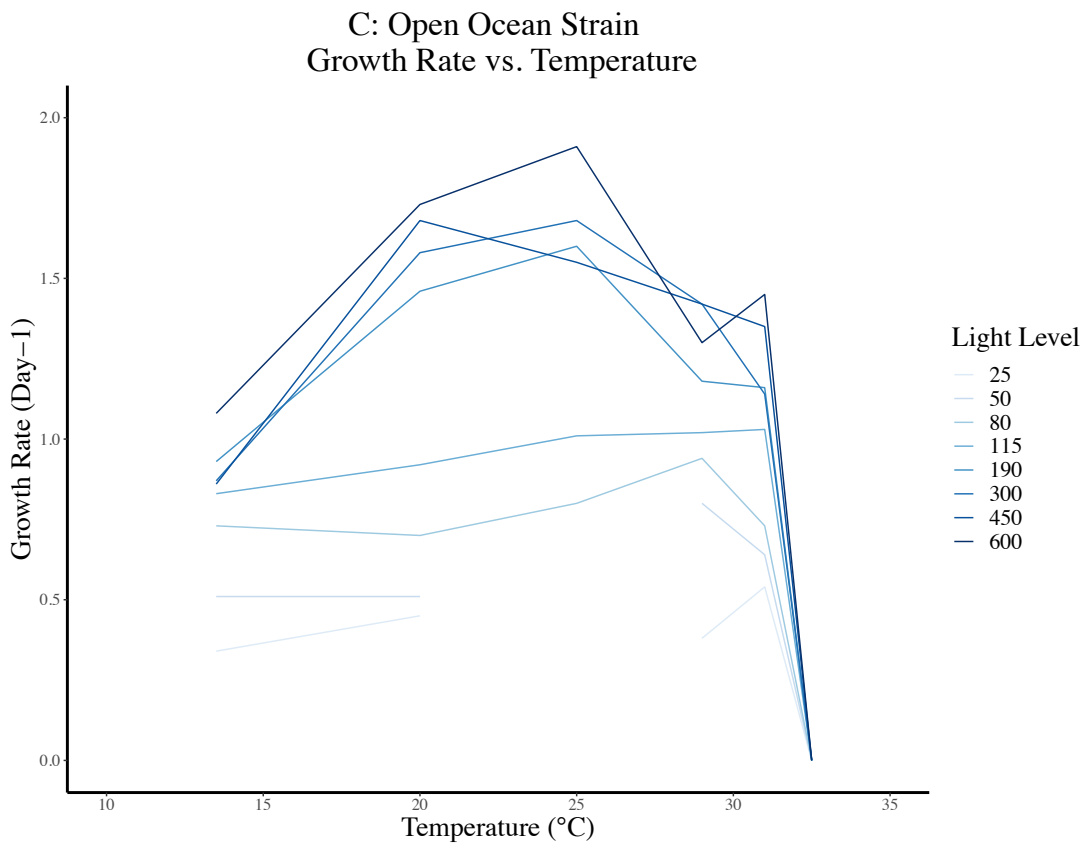


**Figure 5C.** Growth rates for the open ocean strain as they relate to temperature and irradiance.

**Figure 5D**

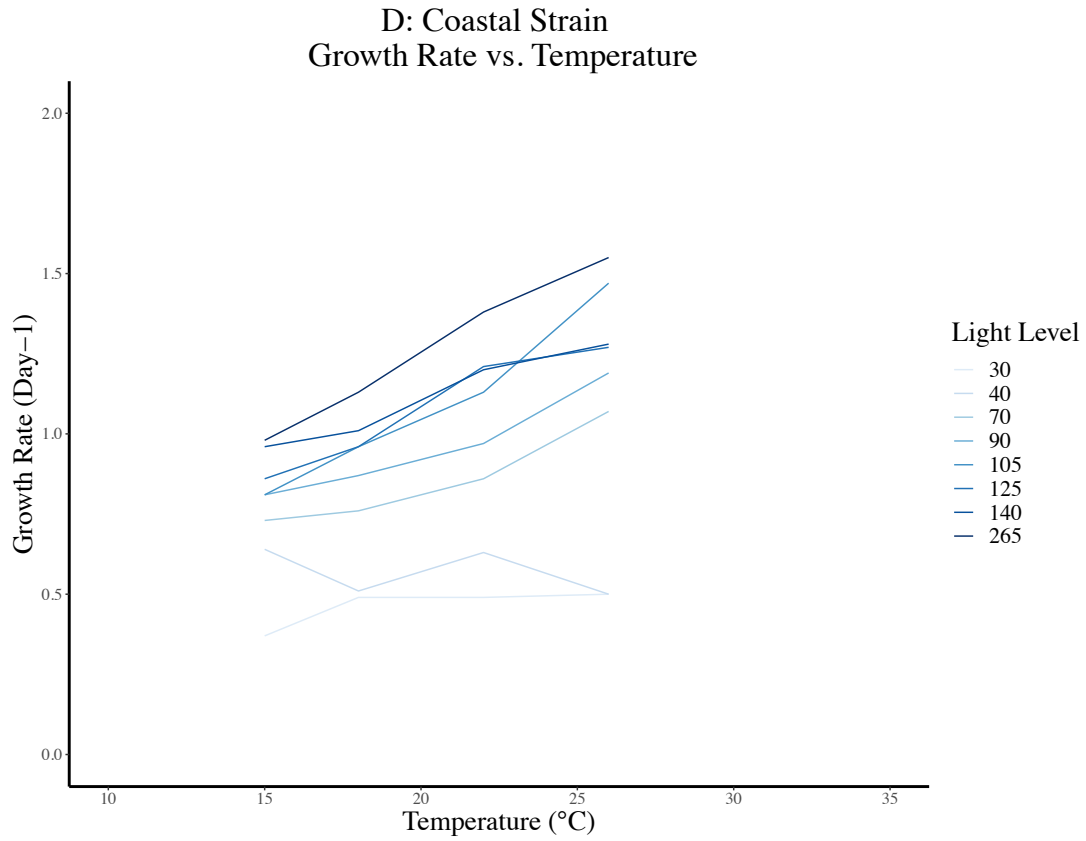


**Figure 5D.** Growth rates for the coastal ocean strain as they relate to temperature and irradiance.

**Figure 6**

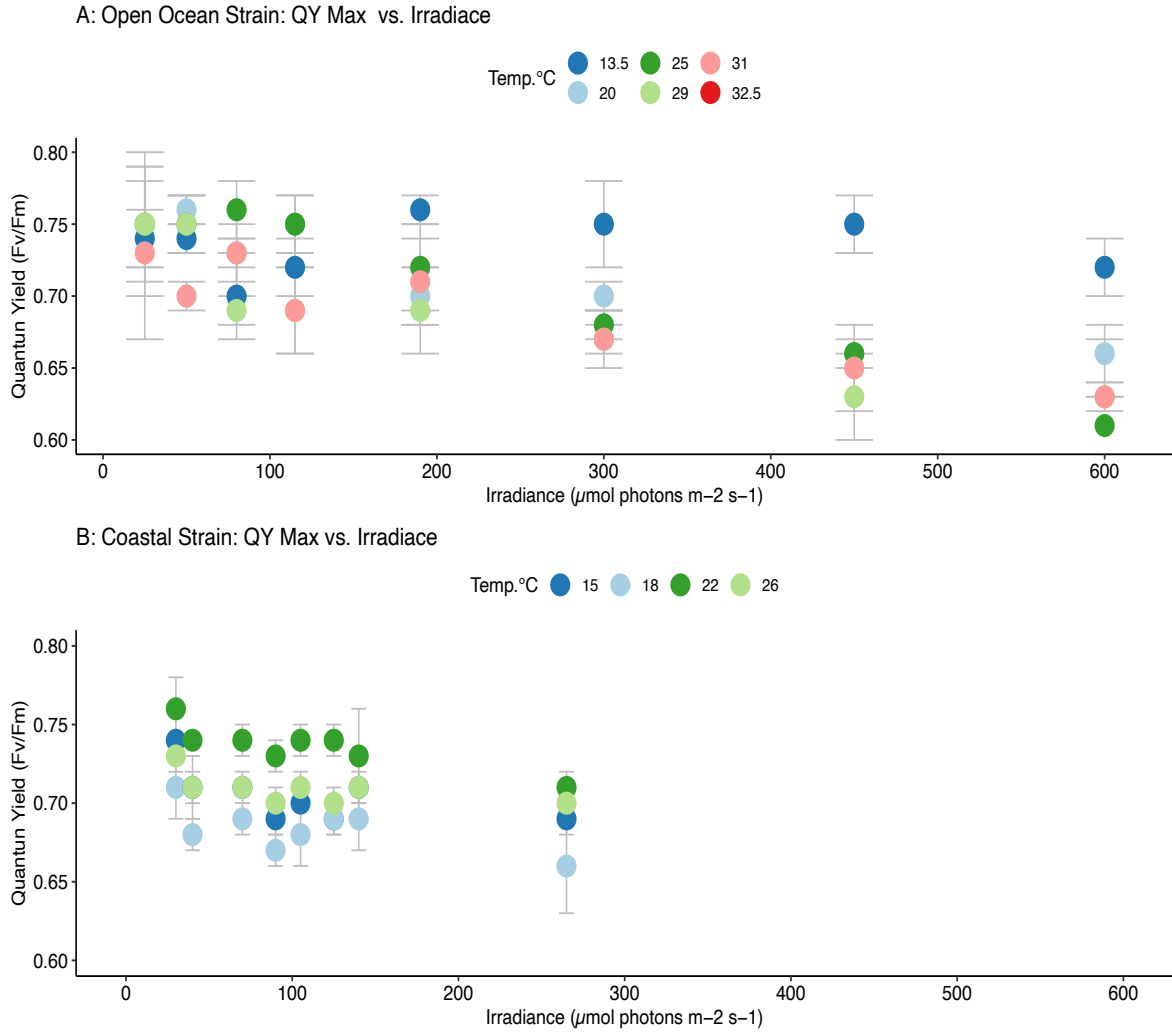


**Figure 6.** Relationship between quantum yield and irradiance for (A) Open ocean strain and (B) Coastal strain

**Figure 7**

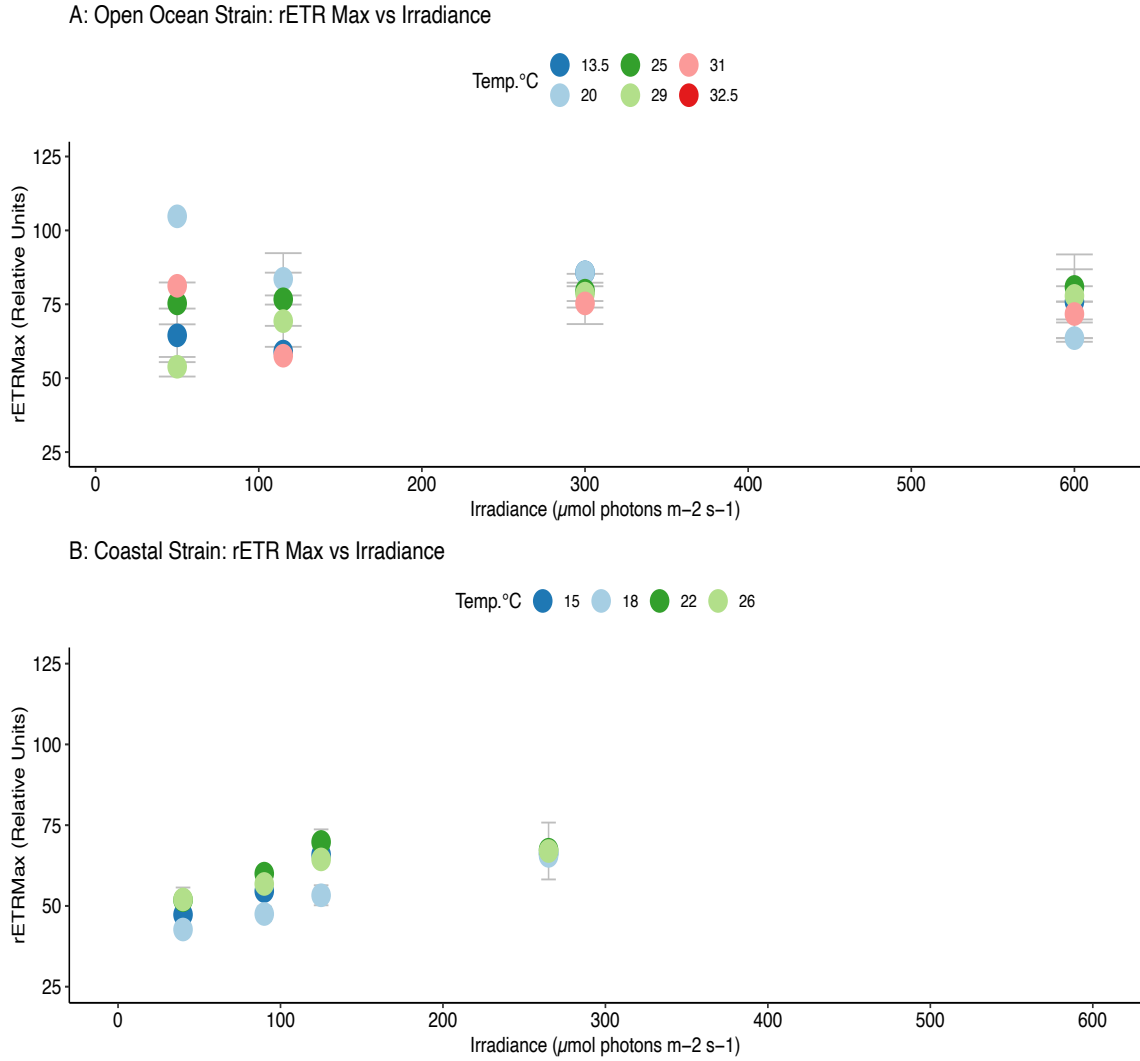


**Figure 7.** Relationship between relative electron transport rates and irradiance for (A) Open ocean strain and (B) Coastal strain

**Figure 8**

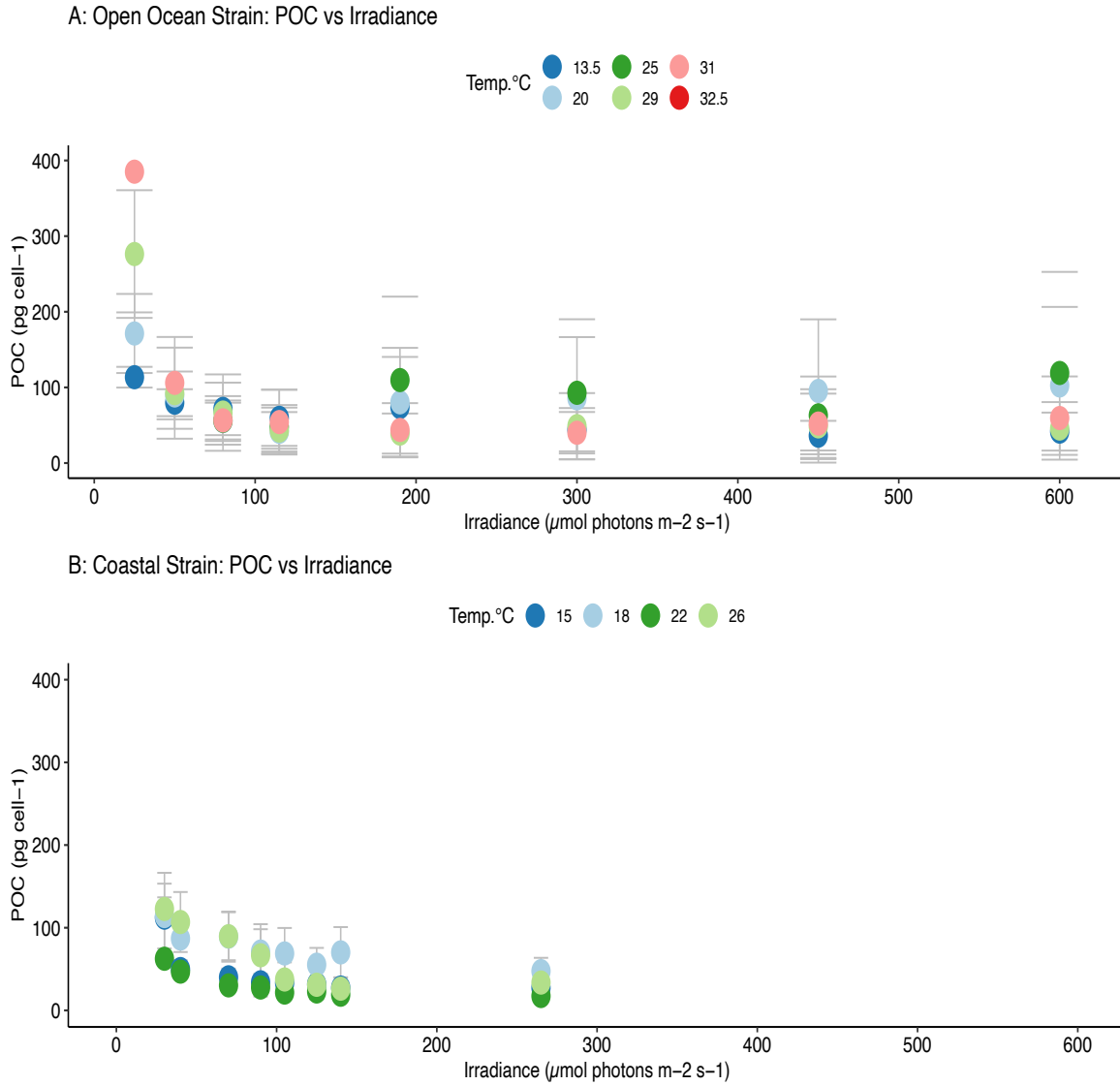


**Figure 8.** Relationship between cellular carbon content and irradiance for (A) Open ocean strain and (B) Coastal strain



**Figure 9**

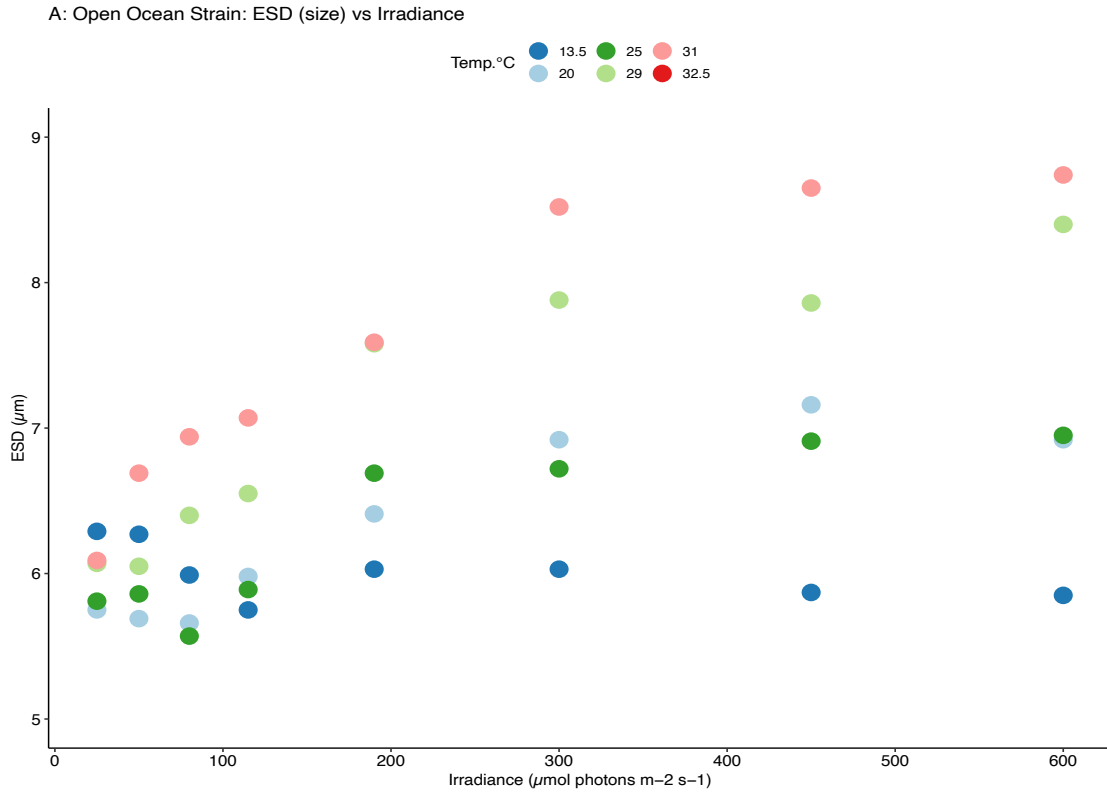


**Figure 9.** Relationship between cell size (ESD) and irradiance for the open ocean strain

**Figure 10**

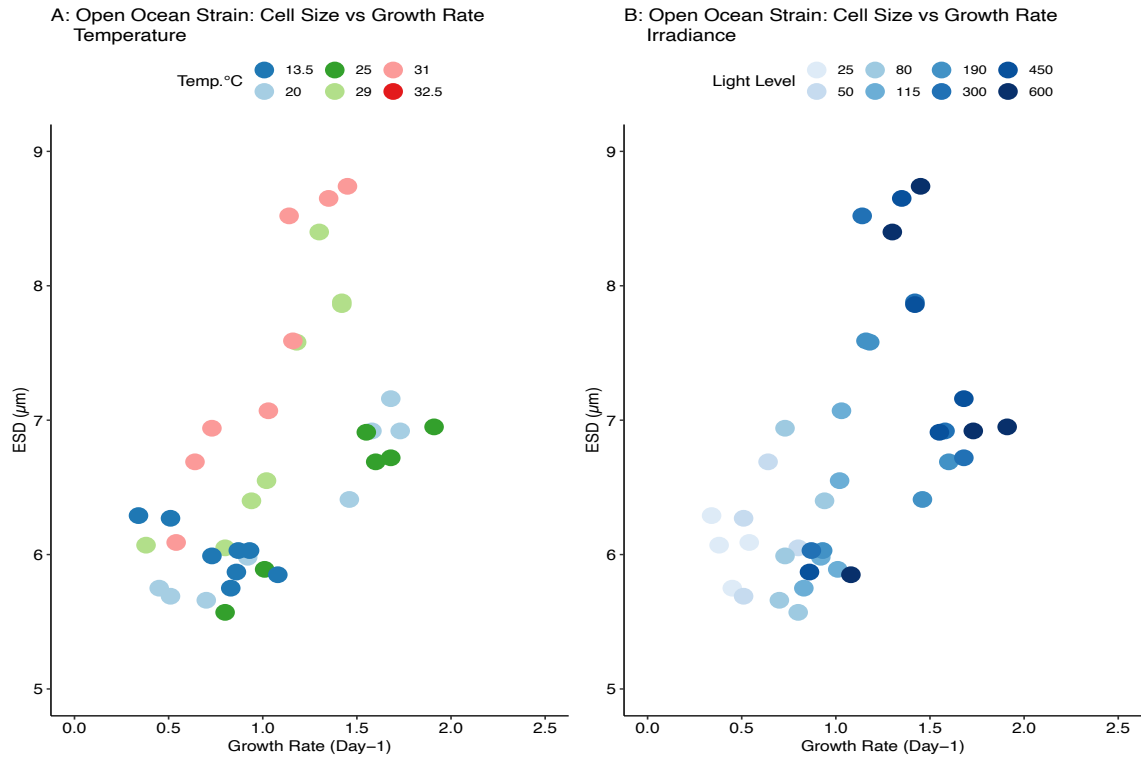


**Figure 10.** Relationship between cell size (ESD) and growth rate for the open ocean strain in terms of temperature (A) and in terms of irradiance (B).

**Figure 11**

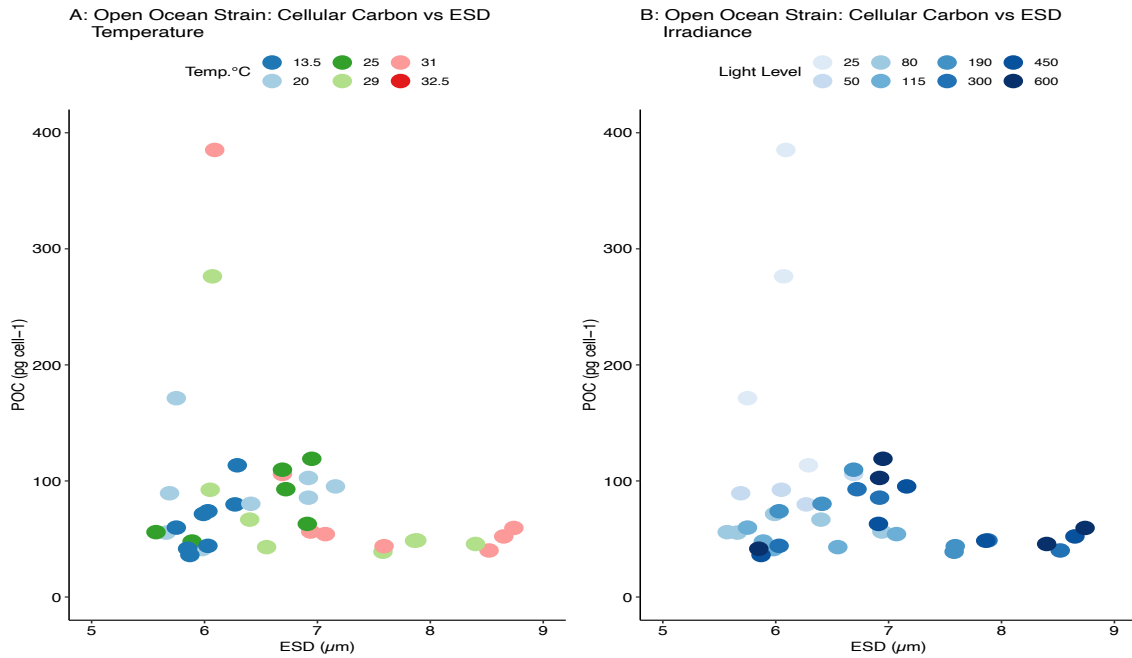


**Figure 11.** Relationship between cell size (ESD) and cellular carbon content for the open ocean strain in terms of temperature (A) and in terms of irradiance (B).

**Figure 12**

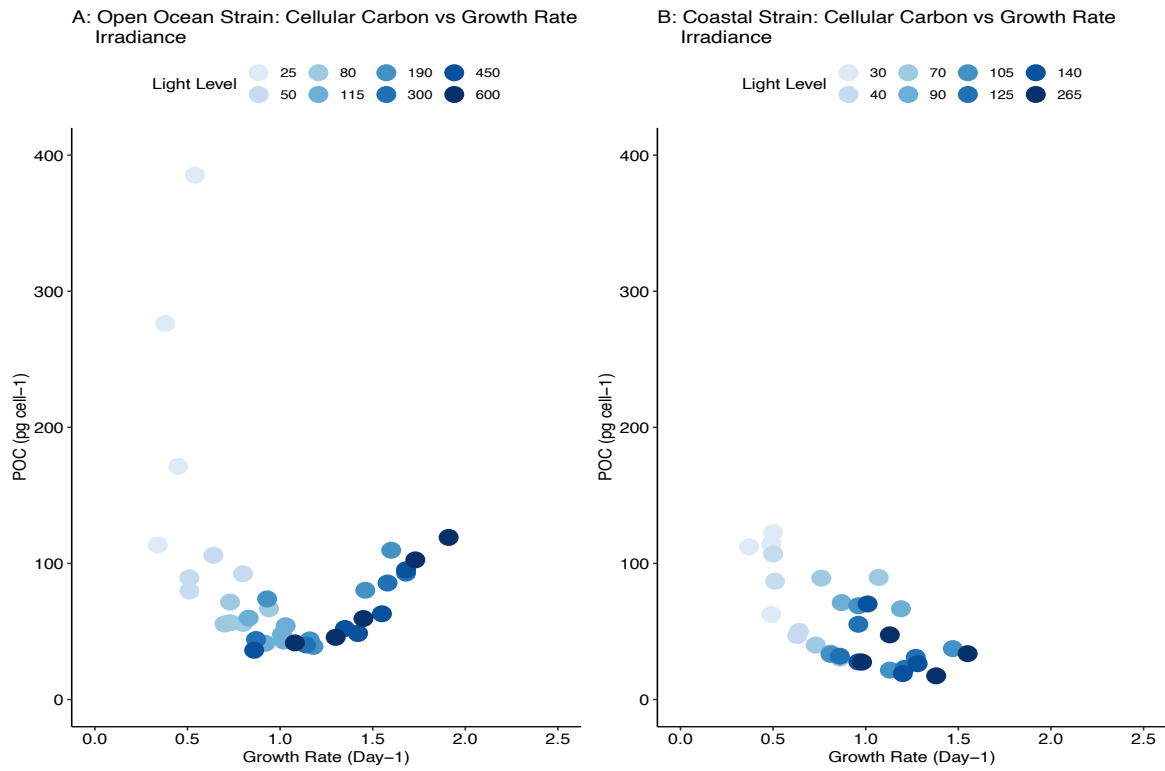


**Figure 12.** Relationship between cellular carbon content and growth rate for the open ocean strain (A) and the coastal strain (B).

**Table 1**

<b>CCMP 1014 (Open Ocean)</b>		<b>CCMP 1335 (Coastal)</b>	
<b>Temperatures (°C)</b>	<b>Irradiances (<math>\mu\text{mol photons} \cdot \text{m}^{-2} \cdot \text{s}^{-1}</math>)</b>	<b>Temperatures (°C)</b>	<b>Irradiances (<math>\mu\text{mol photons} \cdot \text{m}^{-2} \cdot \text{s}^{-1}</math>)</b>
<b>13.5</b>	<b>25</b>	<b>15</b>	<b>30</b>
<b>20</b>	<b>50</b>	<b>18</b>	<b>40</b>
<b>25</b>	<b>80</b>	<b>22</b>	<b>70</b>
<b>29</b>	<b>115</b>	<b>26</b>	<b>90</b>
<b>31</b>	<b>190</b>		<b>105</b>
<b>32.5</b>	<b>300</b>		<b>125</b>
	<b>450</b>		<b>140</b>
	<b>600</b>		<b>265</b>

**Table 1.** Chart of experimental conditions for each strain of *Thalassiosira pseudonana*

**Table 2**

	<b>Open Ocean Strain (CCMP 1014)</b>	<b>Coastal Strain (CCMP 1335)</b>
<b>Supra Optimal Temperature Range</b>	<b>29 – 31°C</b>	<b>Not reached in this study</b>
<b>Optimal Temperature Range</b>	<b>20 – 25°C</b>	<b>~26°C</b>
<b>Sub Optimal Temperature Range</b>	<b>~13°C</b>	<b>15 – 18°C</b>
<b>Light Saturation</b>	<b>190 <math>\mu\text{mol photons m}^2\text{s}^{-1}</math></b>	<b>125 <math>\mu\text{mol photons m}^2\text{s}^{-1}</math></b>

**Table 2.** Definitions of biologically relevant temperature and irradiance cutoffs based upon the growth rate data from this study

**Table 3**

<b>Parameter</b>	<b>Open Ocean Strain (CCMP 1014)</b>	<b>Coastal Strain (CCMP 1335)</b>
<b>Conditions of highest Growth Rate</b>	<b>25°C 6000 photons m<sup>-2</sup>s<sup>-1</sup></b>	<b>26°C *265 μmol photons m<sup>-2</sup>s<sup>-1</sup></b>
<b>rETR<sub>max</sub></b>	<b>Range = 53.85 – 104.76 Median = 76.30</b>	<b>Range = 42.66 – 69.77 Median = 58.40</b>
<b>Temperature effects below saturating light level</b>	<b>None</b>	<b>Warmer temperatures = higher growth rates</b>
<b>Conditions of highest QY<sub>max</sub></b>	<b>13°C 190 μmol photons m<sup>-2</sup>s<sup>-1</sup></b>	<b>No statistically significant differences with temperature or irradiance</b>
<b>Cell Size (ESD)</b>	<b>Range = 5.6 – 8.7 μm Median = 6.4 μm</b>	<b>Range = 4.6 – 6.6 μm Median = 6.0 μm</b>
<b>Cellular Chl a</b>	<b>Range 0.09 – 0.69 pg Median = 0.28 pg</b>	<b>Range 0.08 – 0.45 pg Median = 0.26 pg</b>
<b>Cellular Carbon</b>	<b>Range 36.2 – 385.2 pg Median = 61.4 pg</b>	<b>Range 17.4 – 122.7 pg Median = 43.5 pg</b>

\* Coastal strain was not tested beyond 265 μmol photons m<sup>-2</sup>s<sup>-1</sup>